

3 TITANIUM GRADE 5

Titanium Grade 5 (Ti-6Al-4V) is very similar to Titanium Grade 24, except that Titanium Grade 24 has the addition of a small amount of palladium (0.04 to 0.08 weight percent) to enhance corrosion resistance properties. The material used in this investigation was obtained from Tricor Industrial, Inc., and chemical analysis by Staveley Services Materials Testing showed that its chemical composition meets the ASTM Standards for Titanium Grade 5 (ASTM International, 2007b). Table 3-1 shows the chemical composition as given by Staveley Services Materials Testing. For Titanium Grade 5, the three main tasks in this investigation involve analysis of creep test data; characterization of the microstructure and texture of the undeformed, as-received plate material; and transmission electron microscopy to identify the creep deformation mechanisms.

3.1 Analysis of Creep Data of Titanium Grade 5

To determine the creep behavior of Titanium Grade 5 under various loading conditions, creep tests were performed at Westmoreland Mechanical Testing and Research, Inc. At 150 °C [302 °F], Titanium Grade 5 specimens were creep tested at various stress levels (given as a percentage of the 0.2 percent yield stress; see Appendix A)—40, 55, 70, 85, and 100 percent yield stress. The duration of the test was 200 hours. The objectives of this analysis are to determine (i) the empirical equations that best describe the creep behavior of Titanium Grade 5 at the various stress levels at 150 °C [302 °F], (ii) the creep constants as a function of stress level at 150 °C [302 °F], and (iii) a minimum stress level at which creep occurs at 150 °C [302 °F].

3.1.1 Determining the Empirical Equation to Describe Creep Data

As described in Section 2.1.1, creep curves can be described by one of two equations: a power-law Eq. (2-1) or a logarithmic form Eq. (2-2). In this analysis of Titanium Grade 5, creep curves were derived using both the power-law and logarithmic type equations to determine which empirical equation describes the data more accurately. The 200-hour creep curves for Titanium Grade 5 at 150 °C [302 °F] at the various stress levels are shown in Figures 3-1 through 3-5, superimposed with the power-law and logarithmic equations that describe the experimental data. The composite creep curve for the various stress levels is shown in Figure 3-6.

The creep curves shown in Figures 3-1 through 3-5 indicate that both the power-law Eq. (2-1) and the logarithmic Eq. (2-2) offer a reasonable fit for the data at the various stress levels. The average of the R^2 value of the five creep curves for the power-law equation is approximately

Carbon	Hydrogen	Iron	Oxygen	Nitrogen	Aluminum	Vanadium	Titanium
0.015 weight percent	67–75 parts per million	0.150 weight percent	0.176 weight percent	0.010 weight percent	6.219 weight percent	4,000 weight percent	Balance

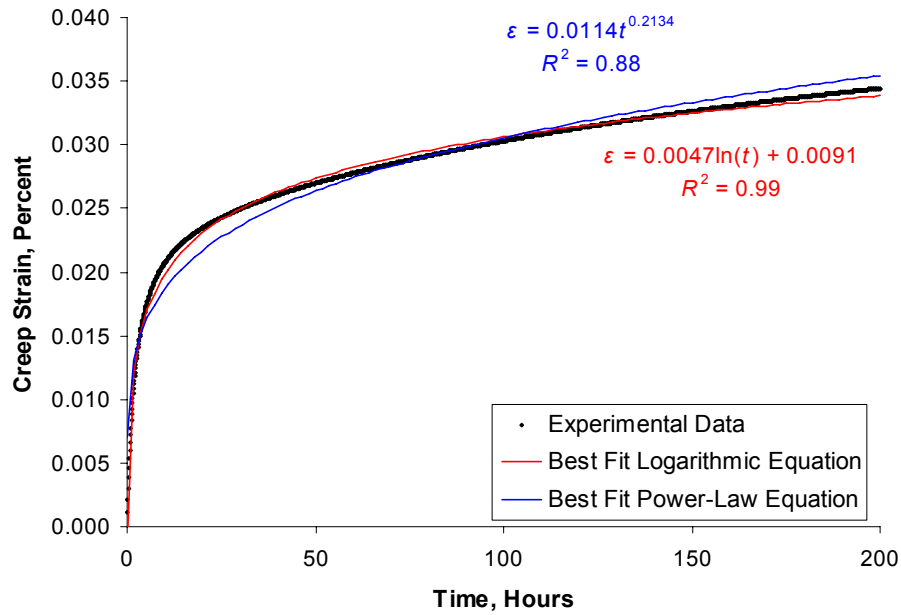


Figure 3-1. Experimental and Analytical Creep Curves for Titanium Grade 5. Stress Level of 40 Percent Yield Stress; Temperature of 150 °C [302 °F].

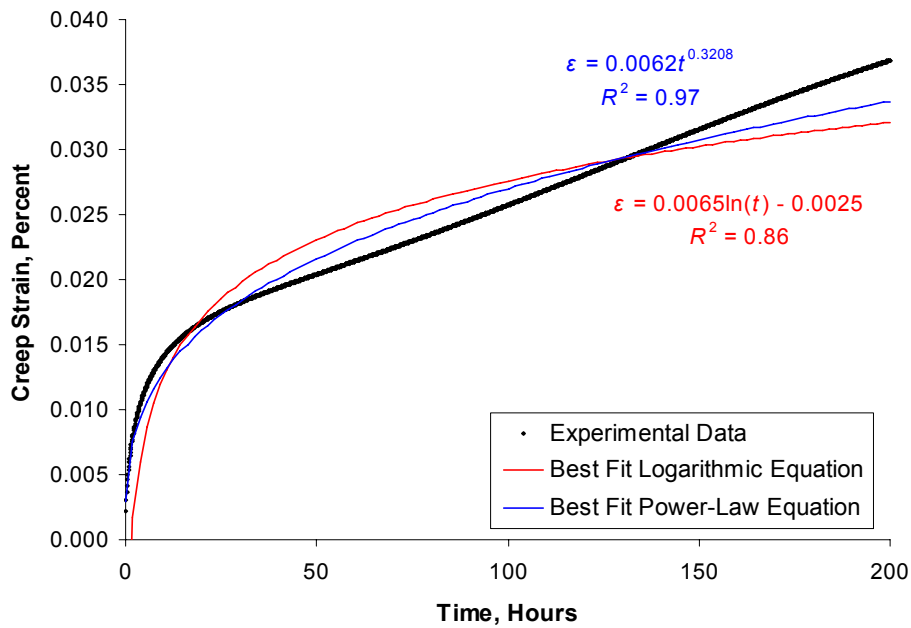


Figure 3-2. Experimental and Analytical Creep Curves for Titanium Grade 5. Stress Level of 55 Percent Yield Stress; Temperature of 150 °C [302 °F].

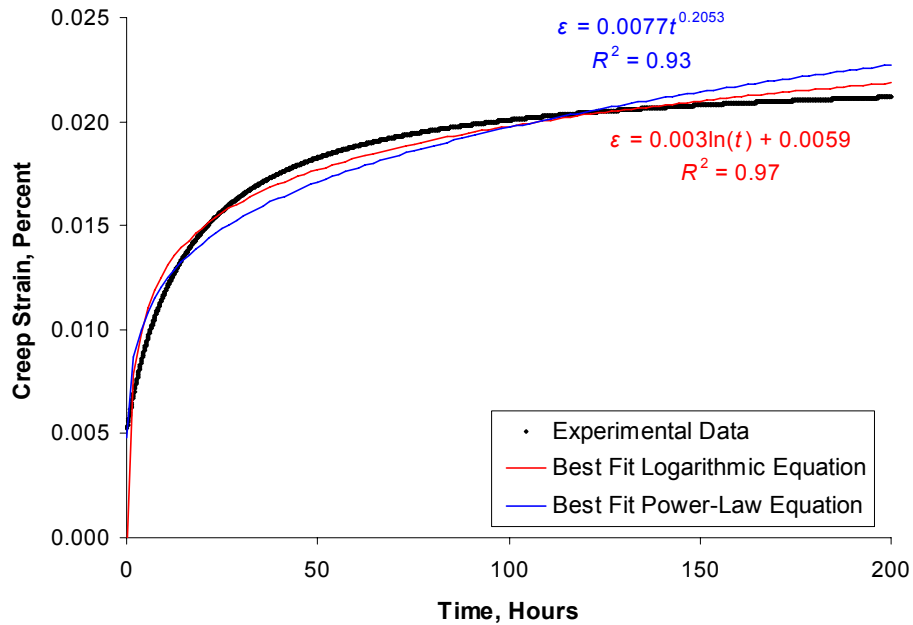


Figure 3-3. Experimental and Analytical Creep Curves for Titanium Grade 5. Stress Level of 70 Percent Yield Stress; Temperature of 150 °C [302 °F].

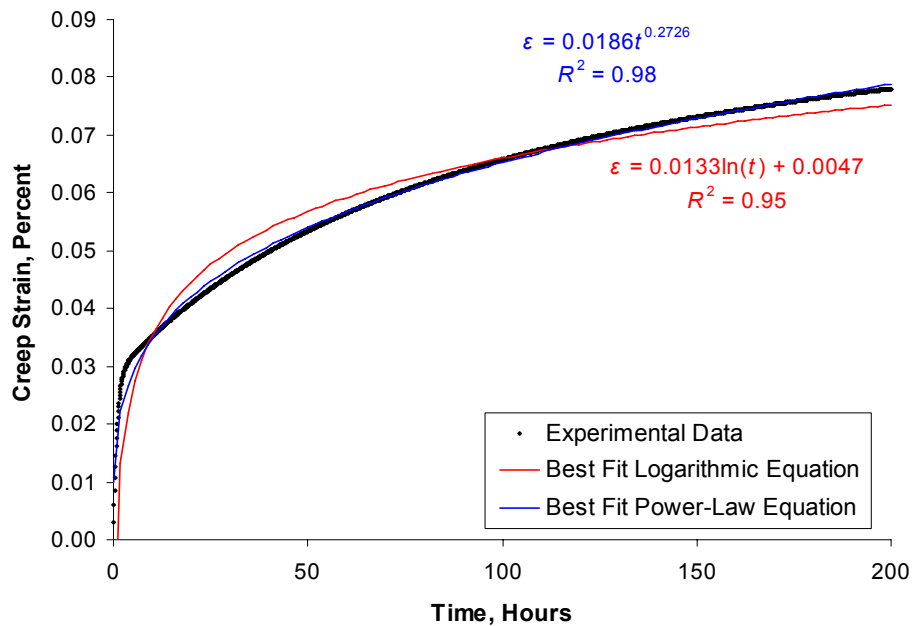


Figure 3-4. Experimental and Analytical Creep Curves for Titanium Grade 5. Stress Level of 85 Percent Yield Stress; Temperature of 150 °C [302 °F].

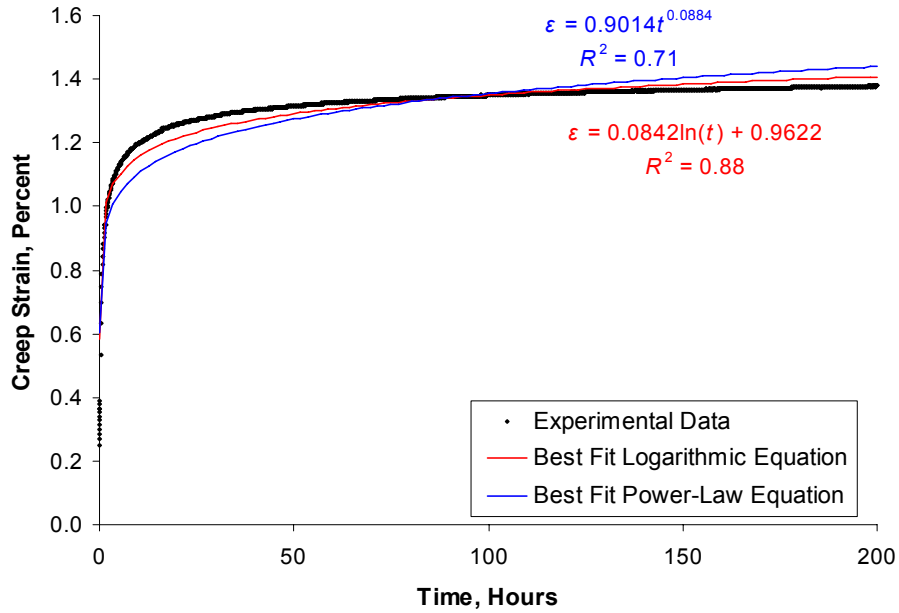


Figure 3-5. Experimental and Analytical Creep Curves for Titanium Grade 5. Stress Level of 100 Percent Yield Stress; Temperature of 150 °C [302 °F].

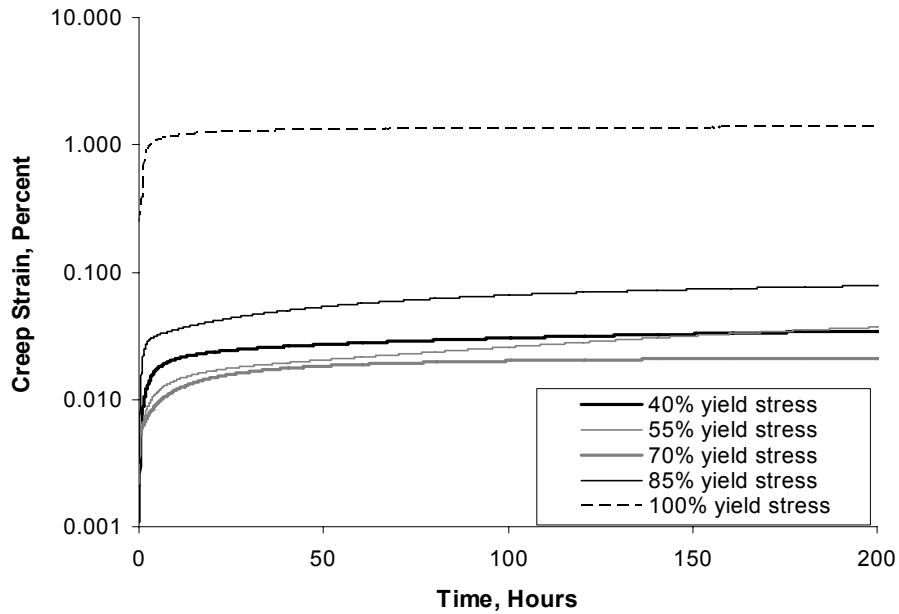


Figure 3-6. Experimental Creep Curves for Titanium Grade 5 at 150 °C [302 °F]

0.89 and for the logarithmic equation is approximately 0.93. Moreover, the logarithmic equation provides the best fit at the highest stress level (100 percent yield stress), when creep strain is most significant. As such, the logarithmic Eq. (2-2) will be used to describe the creep behavior for Titanium Grade 5 at 150 °C [302 °F].

3.1.2 Creep Constants as a Function of Stress Level

Given that the creep behavior for Titanium Grade 5 at 150 °C [302 °F] is best described by a logarithmic Eq. (2-2), the creep constants A' and B can be given as a function of stress level. The values for creep constant A' and B , taken from the fitting empirical equations for the creep curves presented in Figures 3-1 through 3-5, are shown on Figures 3-7 and 3-8 as a function of stress level.

Given the small amount of creep strain at stresses less than 100 percent yield stress, the relationship between the creep constants and stress level is not very strong when compared to that for Titanium Grade 7, particularly for the constant A' . The empirical equations that relate the creep constants to the stress level σ (where σ is the percentage of the 0.2 percent yield stress) are as follows

$$A' = 2.82 \times 10^{-4} e^{0.05920\sigma} \quad (3-1)$$

$$B = 4.87 \times 10^{-4} e^{0.04325\sigma} \quad (3-2)$$

Substituting Eqs. (3-1) and (3-2) into Eq. (2-2) gives a general expression for the effect of stress level on creep strain for Titanium Grade 5 at 150 °C [302 °F], as follows

$$\varepsilon = 2.82 \times 10^{-4} e^{0.05920\sigma} + 4.87 \times 10^{-4} e^{0.04325\sigma} \ln(t) \quad (3-3)$$

3.1.3 Threshold Stress for Creep Deformation of Titanium Grade 5

Previous investigations on creep of Titanium Grade 5 at low temperatures provided varying results: Imam and Gilmore (1979) reported that Titanium Grade 5 creeps at stresses as low as 25 percent yield stress, while Riemann (1971) reported no creep at less than 85 percent yield stress. The experimental data from the creep tests performed at Westmoreland Mechanical Testing and Research, Inc. can be used to derive a minimum threshold below which creep deformation is negligible for Titanium Grade 5. It was determined that even at the lowest stress level at which creep testing was performed (40 percent yield stress), Titanium Grade 5 exhibited a creep behavior. Therefore, an empirical equation must be developed to describe the extent of creep strain as a function of stress level. As seen in Figure 3-9, an exponential Eq. (3-4) can be used to describe the relationship between strain ε , and stress level, σ (where σ is the percentage of the 0.2 percent yield stress)

$$\varepsilon(\sigma) = 1.75 \times 10^{-3} e^{0.0542\sigma} \quad (3-4)$$

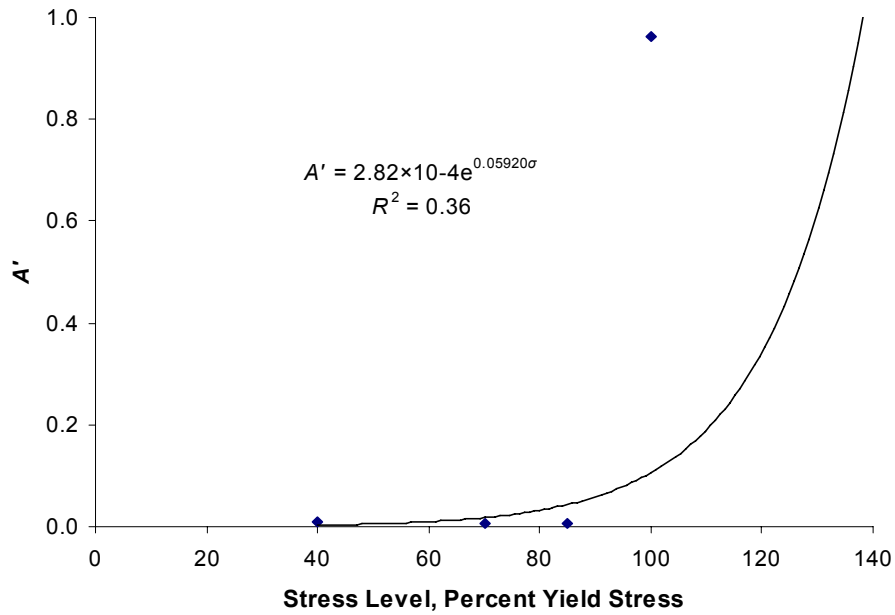


Figure 3-7. The Creep Constant A' as a Function of Stress Level for Titanium Grade 5 Tested at 150 °C [302 °F]

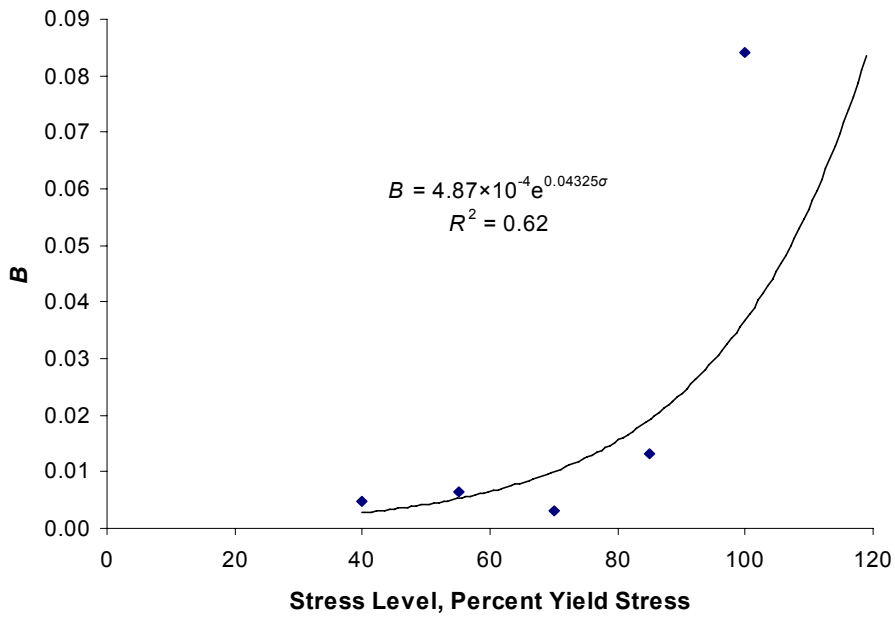


Figure 3-8. The Creep Constant B as a Function of Stress Level for Titanium Grade 5 Tested at 150 °C [302 °F]

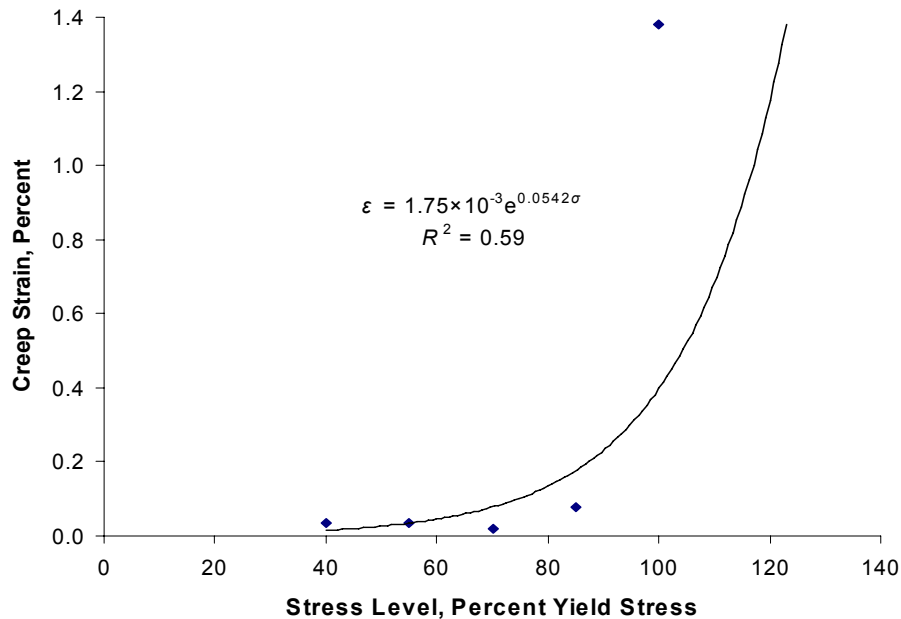


Figure 3-9. A Creep Strain as a Function of Stress Level for Titanium Grade 5 Tested at 150 °C [302 °F]

Due to very low creep strains at stresses less than 100 percent yield stress, the empirical equation that relates creep strain to stress level is not an ideal fit. Recall from Section 2.1.3 that the stress level that corresponds to 0.02 percent strain will be assumed as the stress threshold for creep deformation. Solving Eq. (3-4) for $\epsilon = 0.02$ percent gives a stress threshold of 44.9 percent yield stress. Note that this stress level is above that at which Titanium Grade 5 has been previously reported in this investigation to creep—namely, 40 percent yield stress. However, given that the accuracy of the creep measurement (± 0.02 percent) is a significant fraction of a very small creep strain recorded at 40 percent yield stress (0.0344 percent), the calculated creep stress threshold is a reasonable value.

3.2 Microscopy—Undeformed Titanium Grade 5

An undeformed, as-received plate of Titanium Grade 5 was examined by optical microscopy to characterize the microstructure in terms of grain size and rolling texture.

3.2.1 Procedures

The same experimental procedures as those described in Section 2.2.1 were used to characterize the microstructure of Titanium Grade 7, except that a scanning electron microscope was used instead of an optical microscope due to the small grain size of Titanium Grade 5.

3.2.2 Results

3.2.2.1 Scanning Electron Micrographs

The scanning electron micrographs of the various orientations for the as-received Titanium Grade 5 specimen are shown on Figure 3-10. This alloy was annealed for one hour at 760 °C [1,400 °F]. This type of a heat treatment is called mill annealing and will lead to a microstructure with alternating layers (bands) of equiaxed grains with transformed β grains and elongated a grains with intergranular β grains (Wanjara and Jahazi, 2005).

3.2.2.2 Average Grain Size Calculations

The average grain size for the as-received Titanium Grade 5 specimen was determined using ASTM Standard E112-96, "Standard Test Methods for Determining Average Grain Size" (ASTM International, 2007a) as described in Section 2.2.1.4. The average grain sizes for the respective orientations are summarized in Table 3-2.

3.3 Transmission Electron Microscopy

As described in Section 2.3, transmission electron microscopy is used to characterize the crystallographic structure of a material and identify deformation products in the creep-tested material. The same procedures as those for Titanium Grade 7 were followed for Titanium Grade 5 with the exception of the electrolyte being used to prepare the specimens by jet polishing (see Section 2.3.1.1). For Titanium Grade 5, the specimens were prepared in a solution of 84 percent methanol, 10 percent butanol, and 6 percent perchloric acid at 10 V.

3.3.1 Undeformed Titanium Grade 5

The two-phase microstructure of Titanium Grade 5 is clearly evident in the transmission electron micrographs taken from the undeformed specimen. Figure 3-11 is a low-magnification image showing alternating regions of the α (dark) and β (light) phases. Figure 3-12 is a higher magnification image showing the respective phases. The phases are identified by selected area diffraction. The α -phase and β -phase have different diffraction patterns. Figure 3-13 shows selected area diffraction patterns taken from A and B regions of Figure 3-12. The diffraction pattern in Figure 3-13(a) corresponds to a $\langle 11\bar{2}0 \rangle_{\alpha}$ zone axis, while Figure 3-13(b) corresponds to a $\langle 111 \rangle_{\beta}$ zone axis. Note that this confirms the Burgers orientation relationship (see Appendix B, Section B.2.2) between the respective phases. The undeformed, as-received Titanium Grade 5 shows little evidence of dislocations or any other deformation products.

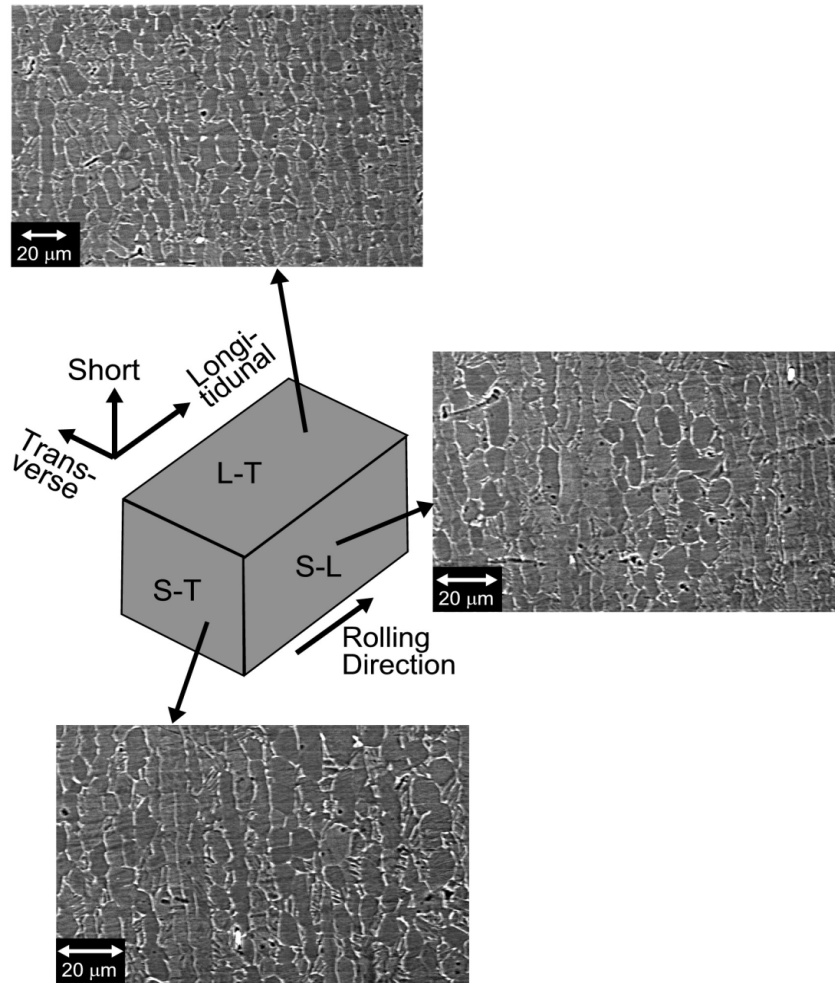


Figure 3-10. Scanning Electron Micrographs of As-Received Titanium Grade 7. Rolling Direction Is Horizontal in all Micrographs. The α -Phase Is Dark and the β -Phase is Light.

Table 3-2. Average Grain Size for As-Received Titanium Grade 5	
Orientation	Average Grain Size, μ m [mil]
Longitudinal-Transverse (L-T)	10.7 [0.42]
Short-Transverse (S-T)	12.3 [0.48]
Short-Longitudinal (S-L)	11.8 [0.46]

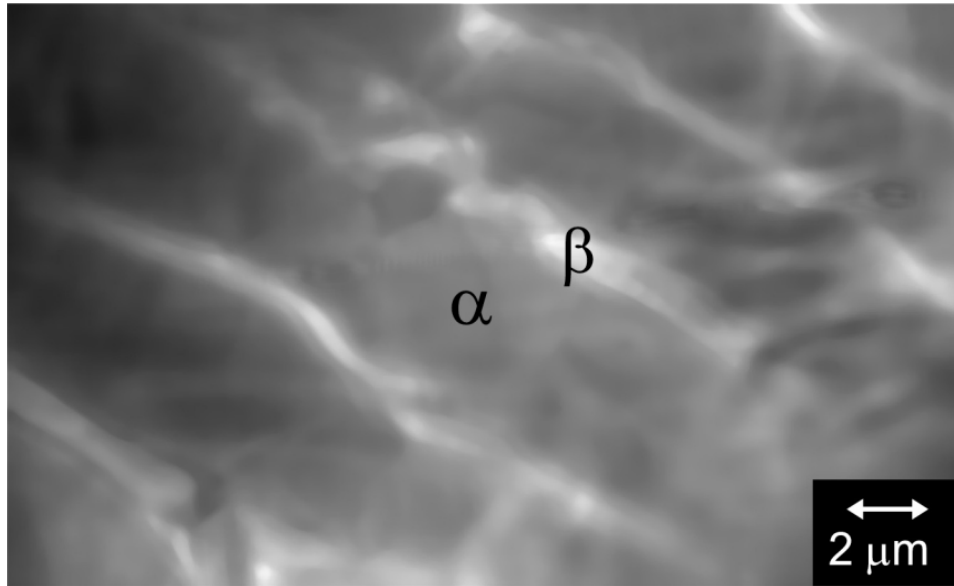


Figure 3-11. Bright-Field Transmission Electron Micrograph of As-Received Titanium Grade 5 Showing Alternating Regions of α -Phase (Dark) and β -Phase (Light)

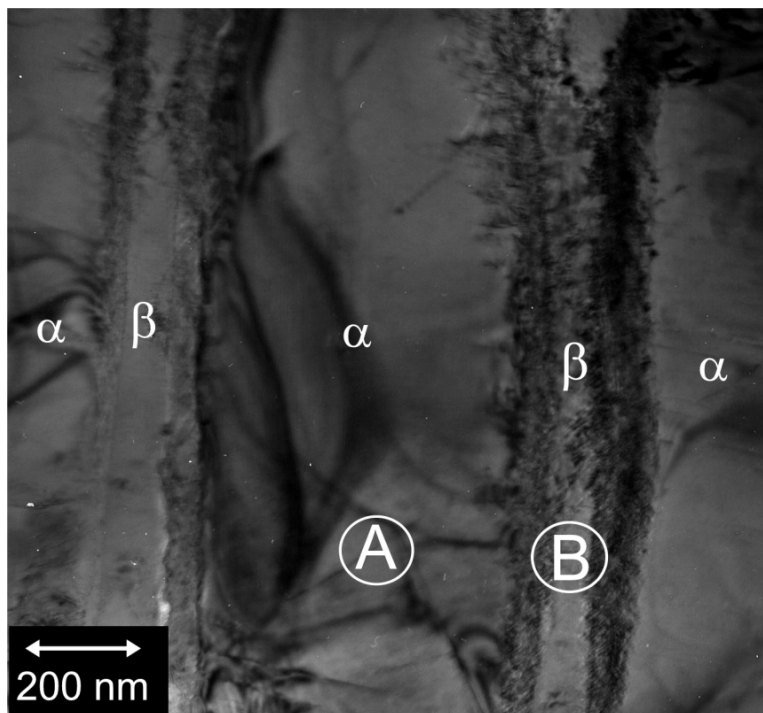


Figure 3-12. Bright-Field Transmission Electron Micrograph of As-Received Titanium Grade 5 Showing Alternating α and β Regions. “A” and “B” Indicate Areas From Which the Selected Area Diffraction Patterns in Figure 3-13 Were Taken.

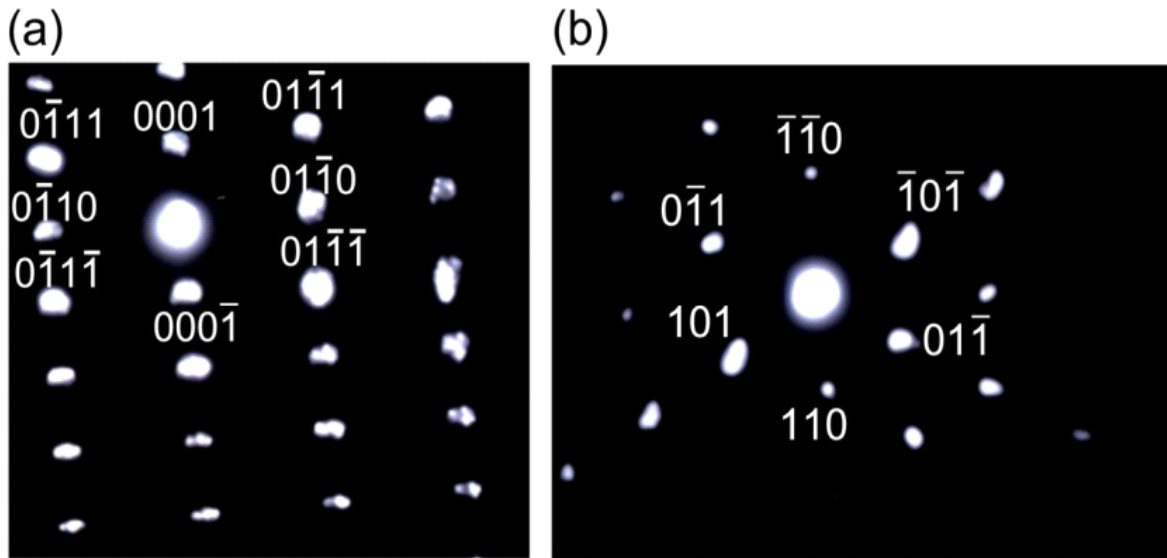


Figure 3-13. Selected Area Diffraction Patterns of As-Received Titanium Grade 5 Taken From the Areas shown in Figure 3-12. (a) Diffraction Pattern of the α -Phase Taken From the Region Marked “A” in Figure 3-12, the Zone Axis Is $\langle 11\bar{2}0 \rangle_{\alpha}$. (b) Diffraction Pattern of the β -Phase From the Region Marked “B” in Figure 3-12; the Zone Axis Is $\langle 111 \rangle_{\beta}$.

3.3.2 Creep-Deformed Titanium Grade 5

The creep-deformed Titanium Grade 5 specimens tested at various stress levels at a constant temperature of 150 °C [302 °F] and at different temperatures at a constant stress level of 85 percent yield stress were examined by transmission electron microscopy to identify the deformation mechanisms (i.e., slip and twinning). Specimens were sectioned from the deformed region of the creep-tested gage length.

3.3.2.1 Transmission Electron Microscopy of Specimens Tested at 150 °C [302 °F]

3.3.2.1.1 Specimen Tested at 100 Percent Yield Stress

The specimen tested at 100 percent yield stress deformed to a creep strain of approximately 1.38 percent after 200 hours. The transmission electron microscopy investigation indicates that slip is the predominant deformation mechanism. Previous investigations (Peters and Luetjering, 1980; Follansbee and Gray, 1989), have suggested that the hexagonal close-packed α -grains dominate the mechanical behavior of Titanium Grade 5 due to the high volume fraction of α in this alloy. At low temperatures (less than 25 percent of the melting temperature), the

predominant deformation mechanism in α -grains of Titanium Grade 5 has been identified as planar slip on prism, basal, and pyramidal planes. Figure 3-14 is a transmission electron micrograph of a-type prism slip, $\bar{b} = \frac{1}{3}\langle 11\bar{2}0 \rangle$, gliding on prism $\{1\bar{1}00\}$ planes in the α -phase of this specimen.

While the mechanical behavior of Titanium Grade 5 is dominated by the α -phase, the β -phase will also be deformed during creep. Previous investigations showed the transmission of slip across the α - β interface during low temperature creep of two-phase Titanium alloy. In this regard, it has been found that the orientation of the respective phases is the critical factor. Suri, et al. (1999) performed creep tests on α - β titanium alloys where the α and β phases were oriented such a way that the slip systems in the respective phases were either aligned or misaligned. Where the slip systems were aligned, dislocations could easily cross the α - β interface and the alloy crept extensively. Where the slip systems of the respective phases were misaligned, dislocations in the α -phase could not easily cross the α - β interface, and instead piled up at that location. This alloy showed high creep resistance. Given the Burgers orientation relationship for the α and β phases in Titanium Grade 5, a prism slip system in the α -phase should be able to easily transmit slip across the α - β interface. Moreover, where slip has been found to cross the α - β interface (Suri, et al., 1999), the operative slip system in the β -phase has been identified as the $\langle 11\bar{1} \rangle \{1\bar{2}\bar{1}\}_\beta$ system. Figure 3-15 is

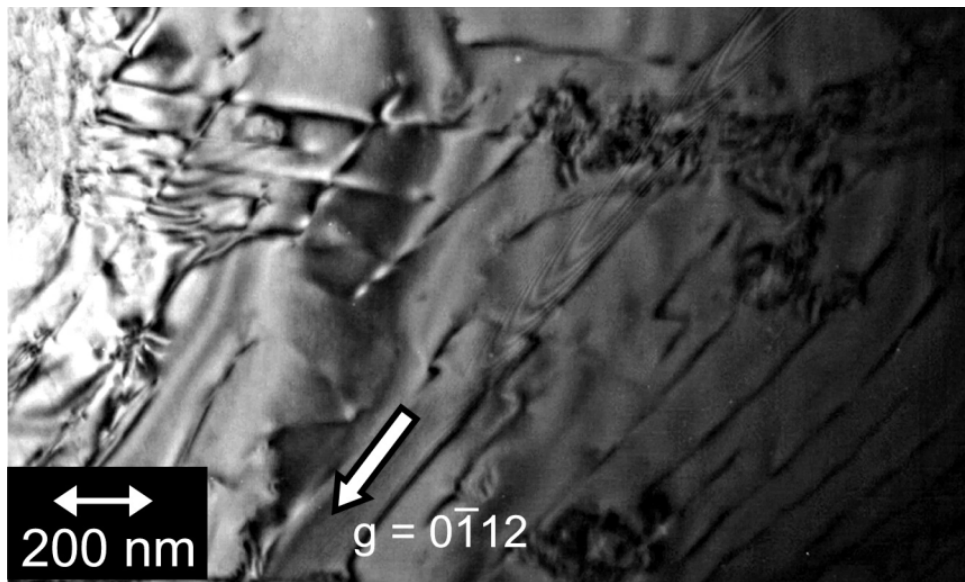


Figure 3-14. Bright-Field Transmission Electron Micrographs of an Array of a-Type Prism Dislocations in Titanium Grade 5 Creep Deformed at 100 Percent Yield Stress at 150 °C [302 °F]

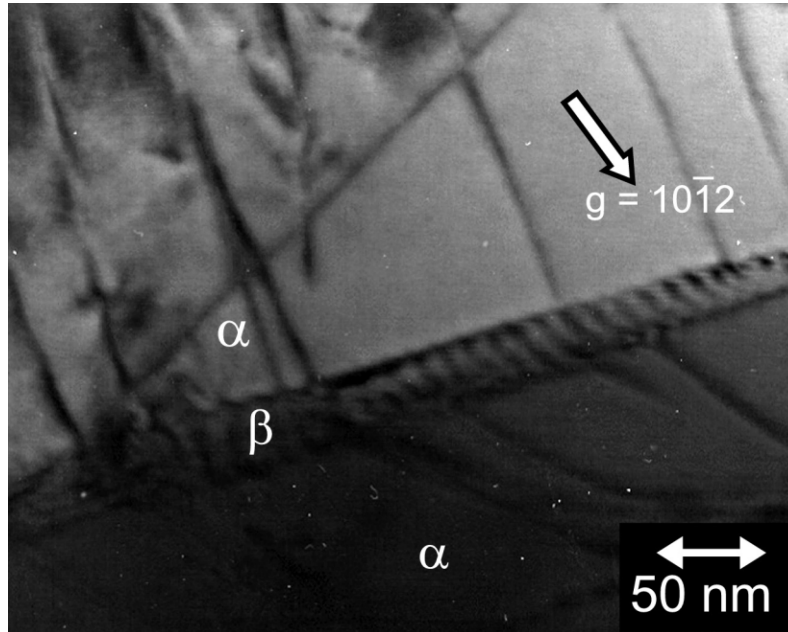


Figure 3-15. Bright-Field Transmission Electron Micrographs of an Array of $\langle 11\bar{1} \rangle \{1\bar{2}\bar{1}\}_{\beta}$ Dislocations in the β -Phase of Titanium Grade 5 Creep Deformed at 100 Percent Yield Stress at 150 °C [302 °F]

a transmission electron micrograph that shows these dislocations in the β -phase for this specimen.

3.3.2.1.2 Specimen Tested at 85 Percent Yield Stress

The Titanium Grade 5 specimen tested at 85 percent yield stress at 150 °C [302 °F] crept to a strain of approximately 0.078 percent after 200 hours. The predominant deformation mechanism for the alloy in these conditions was found to be planar *a*-type slip, $\bar{b} = \frac{1}{3}\langle 11\bar{2}0 \rangle$.

The dislocations can be observed as arrays in the transmission electron micrographs in Figures 3-16 and 3-17. No deformation product was observed in the β -phase at such a small strain level because the strain in the β -phase can be accommodated solely by elastic deformation (Shelton and Ralph, 1983).

3.3.2.1.3 Specimen Tested at 55 Percent Yield Stress

For Titanium Grade 5 tested at 150 °C [302 °F], the specimen tested at 55 percent yield stress crept to a strain of 0.037 percent—more than the specimen tested at 70 percent yield stress, which crept to a strain of 0.021 percent. Because it would be more difficult to find deformation products in the specimen tested at 70 percent yield stress, the specimen tested at 55 percent yield stress was examined by transmission electron microscopy. Dislocation arrays were

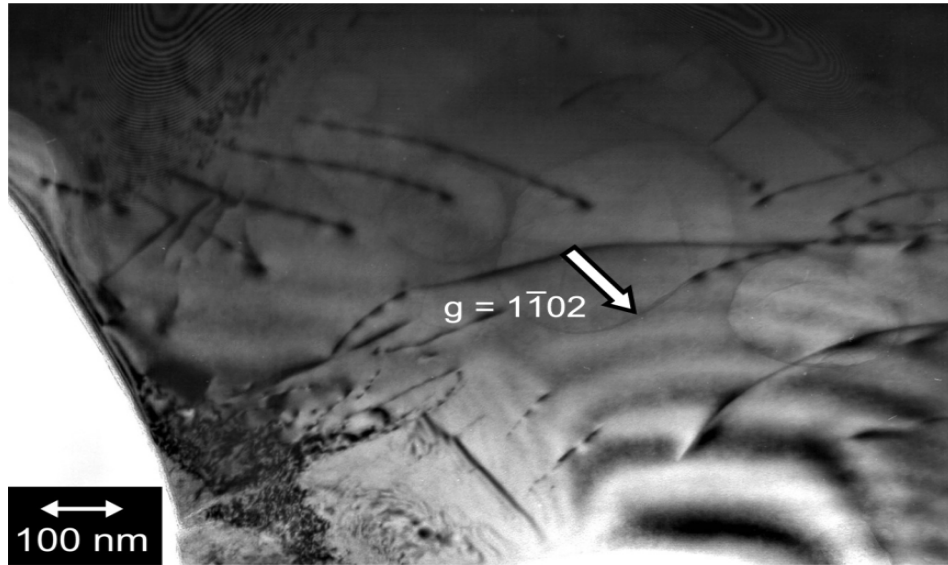


Figure 3-16. Bright-Field Transmission Electron Micrograph of α -Type Prism Dislocations in the α -Phase of Grade 5 Titanium Creep Deformed at 85 Percent Yield Stress at 150 °C [302 °F]

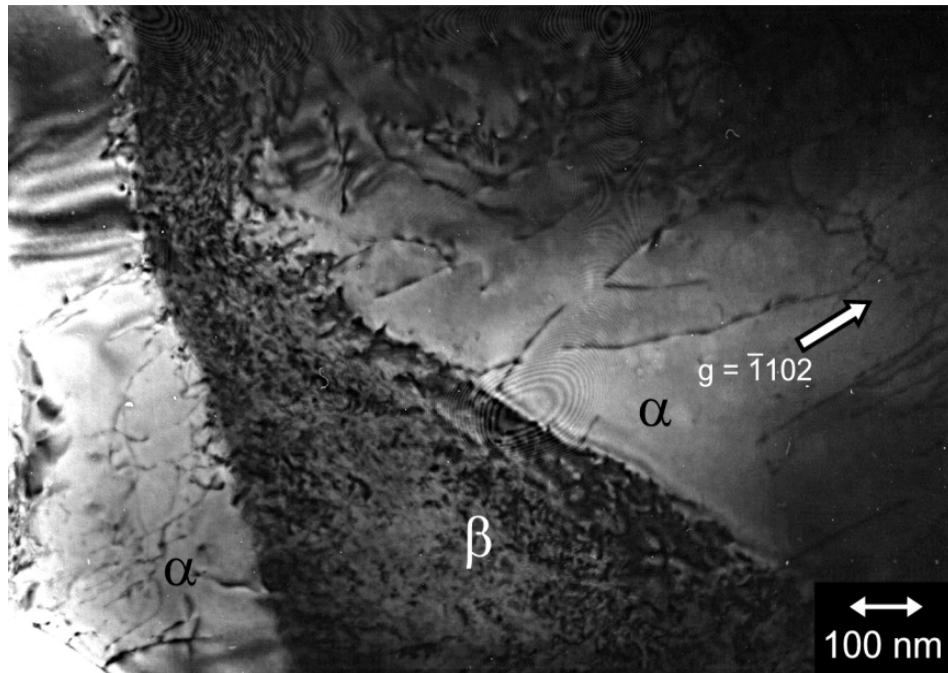


Figure 3-17. Bright-Field Transmission Electron Micrograph of α -Type Prism Dislocations in the α -Phase of Grade 5 Titanium Creep Deformed at 85 Percent Yield Stress at 150 °C [302 °F]. The Dislocations Are in the α -Phase on Both Sides of the β -Region.

difficult to find in this specimen. However, an example of *a*-type slip, $\bar{b} = \frac{1}{3}\langle 11\bar{2}0 \rangle$, is shown in Figure 3-18. No deformation products were found in the β -phase.

3.3.2.1.4 Specimens Tested at 70 and 40 Percent Yield Stress

Given the extremely limited strain of the Titanium Grade 5 specimens creep tested at 70 and 40 percent yield stress, these specimens were not examined with transmission electron microscopy. It would be very difficult to identify and characterize the deformation mechanisms. It is likely, however, that as in the case for the specimens tested at higher stress levels, *a*-type slip in the α -phase is the predominant deformation mechanism.

3.3.2.2 Transmission Electron Microscopy of Specimens Tested at 85 Percent Yield Stress

3.3.2.2.1 Specimen Tested at 250 °C [482 °F]

The specimen tested at 85 percent yield stress at 250 °C [482 °F] crept to a strain of 0.050 percent after 200 hours. In a previous transmission electron microscopy investigation of the deformation behavior of Titanium Grade 5, Follansbee and Gray (1989) found that increasing the temperature of deformation above 200 °C [392 °F] altered the dislocation morphology from planar slip bands to a less coarse planar slip with random dislocation tangles.

The tendency toward random dislocation arrangements with increased temperature suggests that the stress for dislocation motion on the various slip planes becomes comparable, which results in a more active slip system. This morphology is evident in the transmission electron micrographs of Figure 3-19, which show *a*-type dislocations in the α -phase of the Titanium Grade 5 specimen tested at 85 percent yield stress at 250 °C [482 °F]. No deformation products were found in the β -phase because the strain can be accommodated elastically.

3.3.2.2.2 Specimen Tested at 150 °C [302 °F]

Results for the specimen tested at 85 percent yield stress at 150 °C [302 °F] are presented in Section 3.3.2.1.2.

3.3.2.2.3 Specimen Tested at 100 °C [212 °F]

The specimen tested at 85 percent yield stress at 100 °C [212 °F] crept to a strain of 0.064 percent after 200 hours. The predominant deformation mechanism in these conditions is *a*-type planar slip in the α -phase, as seen in Figure 3-20. No deformation products were found in the β -phase.

3.3.2.2.4 Specimen Tested at 25 °C [77 °F]

The specimen tested at 85 percent yield stress at 25 °C [77 °F] crept to a strain of 0.037 percent after 200 hours. The predominant deformation mechanism in these conditions is *a*-type planar

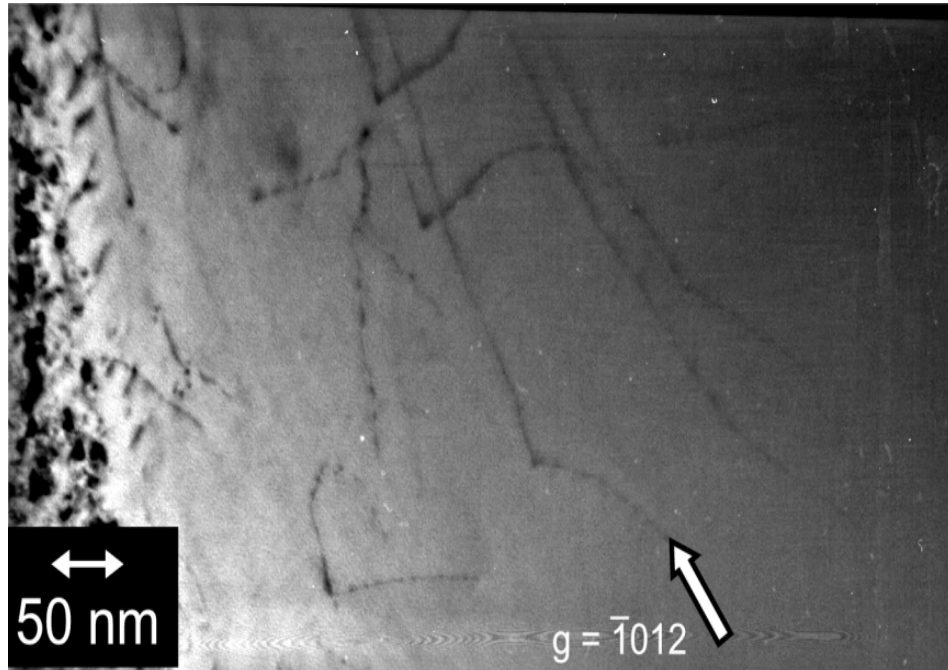


Figure 3-18. Bright-Field Transmission Electron Micrograph of α -Type Prism Dislocations in the α -Phase of Titanium Grade 5 Creep Deformed at 55 Percent Yield Stress at 150 °C [302 °F]

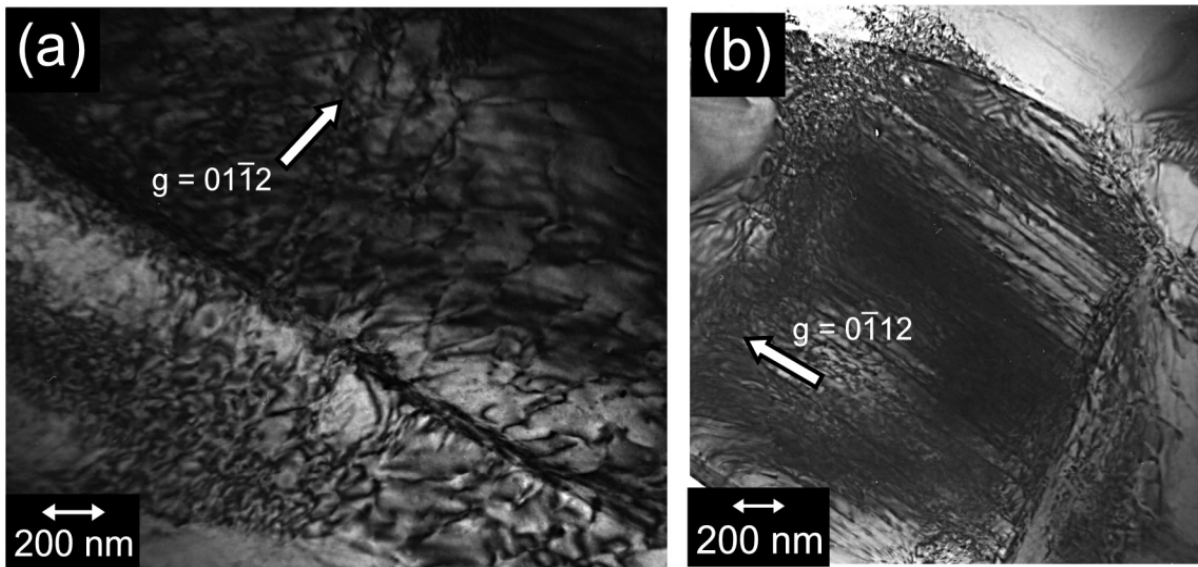


Figure 3-19. Bright-Field Transmission Electron Micrographs of Titanium Grade 5 Creep Deformed at 85 Percent Yield Stress at 250 °C [482 °F]. The Micrographs Show Less Coarse Planar Slip and Random Dislocation Tangles.

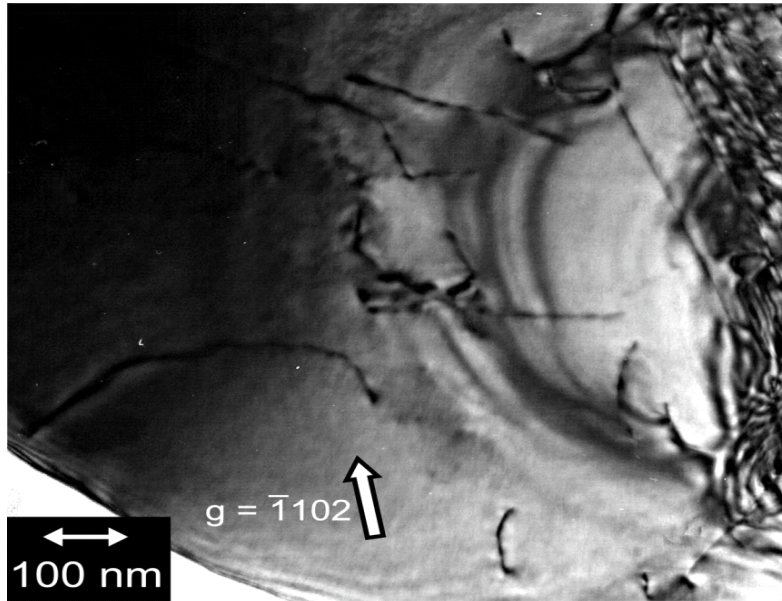


Figure 3-20. Bright-Field Transmission Electron Micrograph of a -Type Dislocations in the α -Phase of Titanium Grade 5 Creep Deformed at 85 Percent Yield Stress at 100 °C[212 °F].

slip in the α -phase, as seen in Figure 3-21. Dislocations in the α -phase are seen on either side of a β -lath. No deformation products were found in the β -phase.

3.4 Summary of the Results for Titanium Grade 5

The three-part study for Titanium Grade 5 that included the analysis of the creep curves, the characterization of the microstructure of the as-received plate material, and the transmission electron microscopy investigation of the creep deformed specimens revealed the effect of microstructure, temperature, and stress level on the creep behavior of this material.

The microstructure of a two-phase $\alpha - \beta$ titanium alloy has a significant effect on the mechanical properties. Depending on the heat treatment and, hence, microstructure, the mechanical properties of the same alloy can differ by 20 percent or more (Boyer, et al., 1994). For instance, in an alloy with small grain size, there is little room for the dislocations to glide before they encounter a boundary. As such, the alloy will show higher strength than an alloy with a large grain size. Scanning electron microscopy of the as-received Titanium Grade 5 plate material revealed alternating layers of equiaxed α grains with transformed β grains and elongated α grains with intergranular β -phase. The average grain size was determined to be approximately 11 μm [0.43 mil].

Based on the results of the creep tests at various stress levels at 150 °C [302 °F], a logarithmic Eq. (2-2) best describes the creep data for Titanium Grade 5 and the creep strain increases with stress level. This finding is consistent with the results obtained for Titanium Grade 7.

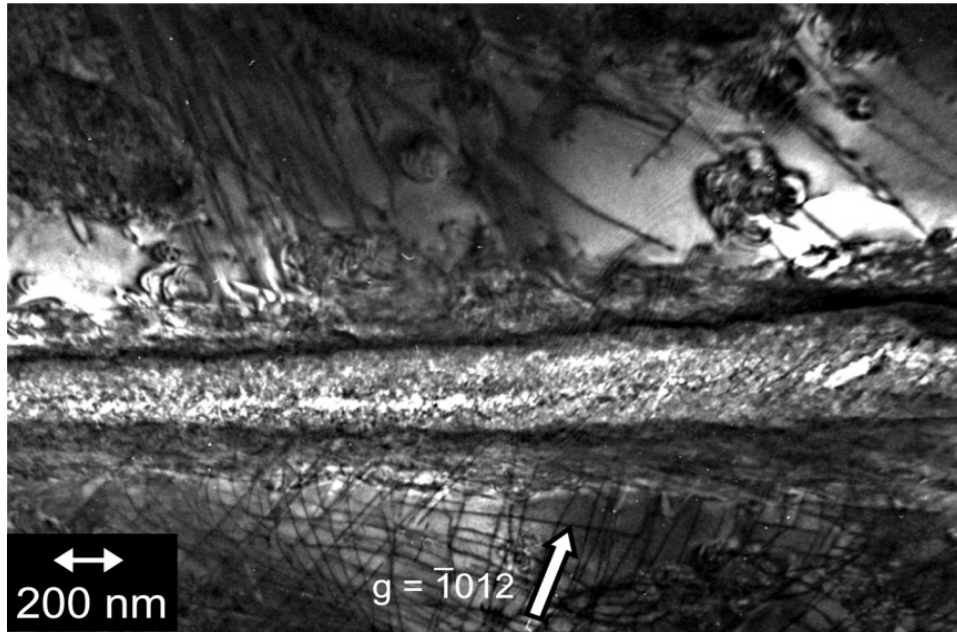


Figure 3-21. Bright-Field Transmission Electron Micrograph of a -Type Dislocations in the α -Phase of Titanium Grade 5 Creep Deformed at 85 Percent Yield Stress at 25 °C [77 °F]

Moreover, the threshold stress for creep was found to be approximately 44.9 percent yield stress. This value has not been previously reported for Titanium Grade 5. The transmission electron microscopy investigation of the specimens tested at the various stress levels revealed that slip in the α -phase is a predominant deformation mechanism at all stress levels. This was confirmed by the measure of the activation energy for creep at 85 percent yield stress, which is consistent with previous investigations for Titanium Grade 5, where slip in the α -phase is the predominant deformation mechanism (de Meester, et al., 1975). The specimen tested at 100 percent yield stress was the most extensively strained and was found to be the only one with slip observed in the β -phase. In the specimens that were tested at lower stress levels, the produced strain was so small that it was accommodated elastically in the β -phase.

4 SUMMARY AND CONCLUSIONS

The creep processes in the engineered barrier are excluded by the U.S. Department of Energy (DOE) based on a low probability screening criterion (Bechtel SAIC Company, LLC, 2004a). On the contrary, the literature review previously performed at the Center for Nuclear Waste Regulatory Analyses indicated that titanium alloys may experience low temperature (less than 25 percent of the melting temperature of the material) creep when subjected to stress levels close to the yield stress for extended period of time (Ankem ans Wilt, 2006). In fact, titanium alloys are known to deform over time, or creep, even when the applied stress level is less than the yield stress (Adenstedt, 1949). This type of behavior may compromise the integrity of the drip shield and diminish its ability to shield the waste package from water seepage. As an outcome, early failure of a drip shield system may result in an increase in the amount of water contacting the waste package. Consequently, this may lead to elevated corrosion rates of the waste package and, potentially, to an increase in the rate of radionuclide mobilization and release. Therefore, it is important to gain insight into creep behavior of titanium alloys DOE is currently considering for the drip shield materials.

This study is the systematic investigation of the creep behavior of Titanium Grade 7 and Grade 5 for the temperature range between 25 and 250 °C [77 and 482 °F] at the stress level ranging from 40 to 100 percent yield stress. Also, it includes the determination of the activation energy necessary for creep deformation, the characterization of the as-received plate microstructures using optical and scanning electron microscopy, and the transmission electron microscopy of the creep specimens. In particular, the creep testing was performed at various stress levels—40, 55, 70, 85, and 100 percent yield stress at 150 °C [302 °F].¹ For this temperature, the empirical equations that best describes the creep behavior were determined. Also at this temperature, the threshold stress for creep (the stress below which creep is considered to be negligible) was calculated. Further, creep testing was performed at 25 °C [77 °F], 50 °C [122 °F] (for Titanium Grade 7 only), 100 °C [212 °F], 150 °C [302 °F], and 250 °C [482 °F] (for Titanium Grade 5 only), at a constant stress level of 85 percent yield stress. Using this creep data, the activation energy for creep was calculated. Because the mechanical properties of titanium alloys are highly dependent on the microstructure (i.e., grain size and morphology), the as-received plate materials were examined by optical and scanning electron microscopy to determine the grain size of Titanium Grade 7 and Grade 5 and whether the materials had any rolling texture. The transmission electron microscopy investigation of the undeformed and creep-deformed material was performed to determine the crystal structure of the alloys and the creep deformation mechanisms.

This investigation showed that it is critical to consider the microstructure and deformation mechanisms, as observed by optical and transmission electron microscopy, when interpreting the data from the creep tests at various temperatures and stress levels to understand the creep behavior of the titanium alloys. Results of the preliminary experimental tests indicated that creep initiation for Titanium Grade 7 and Grade 5 occurs for stresses below the yield stress of a corresponding material for all evaluated temperature. However, the conclusions presented in this report are preliminary. Additional experimental tests on creep behavior of Titanium Grade 7

¹DOE has used material properties associated with a temperature of 150 °C [302 °F] for structural performance assessment of drip shield systems (Bechtel SAIC Company, LLC, 2004b).

and Grade 5 have been initiated to confirm the findings of this study. More explicit conclusions will be offered in future reports.

4.1 Titanium Grade 7

Titanium Grade 7 is a commercially pure titanium alloy with the addition of a small amount of palladium to enhance corrosion resistance properties. The analysis of creep tests performed at various stress levels at 150 °C [302 °F] shows that the creep behavior is best described by a logarithmic equation of the type $\epsilon = A' + B \ln(t)$, where ϵ is creep strain that depends on time t , and A' and B are constants. It was found that the creep constants A' and B increase exponentially with an increase in stress level. The creep strain was plotted as a function of stress level, and it was found that creep strain decreases exponentially as stress level decreases. The threshold stress for creep of Titanium Grade 7 at 150 °C [302 °F] was approximately 32.3 percent yield stress. At a constant stress level of 85 percent yield stress, after the early stage of creep, the creep strain rate of Titanium Grade 7 decreases as the temperature increases above 50 °C [122 °F]. This unusual behavior is attributed to increased twinning activity at lower temperatures and a load drop after yielding at the elevated temperatures. The calculated activation energy for creep of Titanium Grade 7 is consistent with slip-controlled creep at low strains, with a transition to slip and twinning at higher strains for the specimens at room temperature and 50 °C [122 °F].

A plate of as-received Titanium Grade 7 was examined using optical microscopy. The average grain size was found to be approximately 55 μm [2.17 mil]. The grains were equiaxed (have equal axial length), and there was no elongation in the rolling direction.

The transmission electron microscopy investigation of Titanium Grade 7 was used to characterize the crystal structure and identify creep deformation mechanisms. Undeformed specimens were examined to confirm that the alloy had a small number of dislocations in as-received specimens. In addition, creep deformed specimens tested at stress levels of 100, 85, and 70 percent yield stress at 150 °C [302 °F] were examined. The specimen tested at 100 percent yield stress crept significantly, to a strain of approximately 13.7 percent. Slip and twinning were found to be active deformation mechanisms in this specimen. For the specimens tested at the stress levels of 85 and 70 percent yield stress, a -type prism slip was the only observed deformation mechanism, and no twinning was identified. This is likely because of the limited extent of strain at the lower stress levels. Also the specimens tested at 25, 50, and 100 °C [77, 122, and 212 °F] at 85 percent yield stress were examined in this investigation. For the specimens examined at 25 and 50 °C [77 and 122 °F], a -type slip and twinning were found to be active deformation mechanisms, whereas the specimen tested at 100 °C [212 °F] deformed only by a -type slip.

4.2 Titanium Grade 5

Titanium Grade 5 is very similar to Titanium Grade 24. Both are Ti-6Al-4V alloys, with the exception that Grade 24 has a small amount of palladium to enhance corrosion resistance. The analysis of creep tests performed at various stress levels at 150 °C [302 °F] showed that specimens of Titanium Grade 5 exhibit much less creep than Titanium Grade 7. While a Titanium Grade 5 specimen tested at 100 percent yield stress crept to approximately

1.3 percent, the specimens tested at lower stress levels crept to less than 0.1 percent. As such, while the data can be described by logarithmic type equations, the fit obtained for Titanium Grade 5 does not describe data as well as the one obtained for Titanium Grade 7. Although, the findings in regards to the creep constants and creep strain behavior are consistent with the results obtained for Titanium Grade 7. Moreover, the threshold stress for creep of Titanium Grade 5 at 150 °C [302 °F] was found to be approximately 44.9 percent yield stress.

A plate of as-received Titanium Grade 5 was examined by scanning electron microscopy. It was found that the heat treatment of the alloy produced a mill-annealed microstructure of alternating layers (bands) of equiaxed α grains with transformed β grains and elongated α grains with intergranular β grains. Furthermore, the average grain size was found to be approximately 11 μ m [0.43 mil].

The undeformed and creep-deformed Titanium Grade 5 plates were examined to determine the crystallography and the creep deformation mechanisms, confirming that the α and β phases have a Burgers orientation relationship to one another. The mechanical behavior of the creep-deformed specimens is controlled by the α -phase due to the high volume fraction of this phase in Titanium Grade 5. At all temperatures and stress levels, *a*-type slip was identified as the predominant deformation mechanism in the α -phase. At temperatures below 250 °C [482 °F], the dislocation morphology was found to be a coarse planar slip. In the specimen tested at 250 °C [482 °F], the slip was less planar and random dislocation tangles were identified. Further, in all specimens except one tested at 100 percent yield stress at 150 °C [302 °F], no deformation products were identified in the β -phase. Because of the limited strain in these specimens (less than 0.1 percent), the strain can be accommodated elastically in the β -phase. For the specimen tested at 100 percent yield stress at 150 °C [302 °F], the strain was sufficient that dislocations were found in the β -phase.

5 FUTURE WORK

Low temperature creep deformation of Titanium Grade 7 and Grade 5 alloys was investigated for different temperatures and stress levels. This report evaluates creep behavior of these alloys (i) at stress levels of 40, 55, 70, 85, and 100 percent yield stress at the temperature of 150 °C [302 °F] and (ii) at the temperatures of 25, 50, 100, 150, and 250 °C [77, 122, 212, 302, and 482 °F] at the stress level of 85 percent yield stress. These results are useful for developing material behavior predictive models and are beneficial in predicting the long-term life expectancy of the titanium alloys U.S. Department of Energy is currently considering for drip shield materials. However, the result and conclusions presented in this report are preliminary, because only one set of experimental tests data was obtained to date. Additional experimental tests on creep behavior of Titanium Grade 7 and Grade 5 have been initiated to confirm the findings of this study. More explicit conclusions will be offered in future reports.

6 REFERENCES

- Adenstedt, H. "Creep of Titanium at Room Temperature." *Metal Progress*. Vol. 56. pp. 658–660. 1949.
- Aiyangar, A.K., B.W. Neuberger, P.G. Oberson, and S. Ankem. "The Effects of Stress Level and Grain Size on the Ambient Temperature Creep Deformation Behavior of an Alpha-Ti-1.6wt.%V Alloy." *Metallurgical and Materials Transactions A*. Vol. 36A. pp. 637–644. 2005.
- Akhtar, A. "Basal Slip and Twinning in α -Titanium Single Crystals." *Metallurgical Transactions A*. Vol. 6A. pp. 1,105–1,113. 1975.
- Ankem, S. and T. Wilt. "A Literature Review of Low Temperature (<0.25 Tmp) Creep Behavior of α , $\alpha - \beta$, and β Titanium Alloys." San Antonio, Texas: CNWRA. 2006.
- Ankem, S. and H. Margolin. "A Rationalization of Stress-Strain Behavior of Two-Ductile Phase Alloys." *Metallurgical Transactions A*. Vol. 17A. pp. 2,209–2,226. 1986.
- Ankem, S., C.A. Greene, and S. Singh. "Time Dependent Twinning During Ambient Temperature Creep of α -Ti-Mn Alloy." *Scripta Metallurgica et Materialia*. Vol. 15. pp. 803–808. 1994.
- ASTM International. "Standard Test Methods for Determining Average Grain Size." E112–96. West Conshohocken, Pennsylvania: ASTM International. 2007a.
- . "Standard Specification for Titanium and Titanium Alloy Strip, Sheet, and Plate." B265–265b. West Conshohocken, Pennsylvania: ASTM International. 2007b.
- Bechtel SAIC Company, LLC. "FEPs Screening of Processes and Issues, in Drip Shield and Waste Package Degradation." ANL–EBS–PA–000002. Rev. 03. Las Vegas, Nevada: Bechtel SAIC Company, LLC. 2004a.
- . "Seismic Consequence Abstraction." MDL–WIS–PA–000003. Rev. 01. Las Vegas, Nevada: Bechtel SAIC Company, LLC. 2004b.
- Boyer, R., G. Welsch, and E.W. Collings, eds. *Materials Properties Handbook: Titanium Alloys*. Materials Park, Ohio: ASM International. 1994.
- Christian, J.W. and S. Mahajan. "Deformation Twinning." *Progress in Materials Science*. Vol. 94. pp. 1–157. 1995.
- Conrad, H., M. Doner, and B. deMeester. "Critical Review—Deformation and Fracture." *Titanium Science and Technology*. R.I. Jaffee and H.M. Burte, eds. New York City, New York: Plenum Press. pp. 969–1,005. 1973.
- De Meester, B., M. Döner, and H. Conrad. "Deformation Kinetics of the Ti-6Al-4V Alloy at Low Temperatures." *Metallurgical Transactions A*. Vol. 6A. pp. 65–75. 1975.

DOE. DOE/RW-0508, "Viability Assessment of a Repository at Yucca Mountain." Overview and all five volumes. Las Vegas, Nevada: DOE, Office of Civilian Radioactive Waste Management. 1998.

Follansbee, P.S. and G.T. Gray, III. "An Analysis of the Low Temperature, Low and High Strain-Rate Deformation of Ti-6Al-4V." *Metallurgical Transactions A*. Vol. 20A. pp. 863-874. 1989.

Hultgren, C.A., C.A. Greene, and S. Ankem. "Time Dependent Twinning During Ambient Temperature Compression Creep of Alpha-Ti-0.4Mn Alloy." *Metallurgical and Materials Transactions A*. Vol. 30A. pp. 1,675-1,679. 1999.

Imam, M.A. and C.M. Gilmore. "Room Temperature Creep of Ti-6Al-4V." *Metallurgical Transactions A*. Vol. 10A. pp. 419-425. 1979.

Liu, Z. and G. Welsch. "Literature Survey on Diffusivities of Oxygen, Aluminum, and Vanadium in Alpha Titanium, Beta Titanium, and Rutile." *Metallurgical and Materials Transactions A*. Vol. 19A. pp. 1,121-1,125. 1988.

Meyers, M.A., O. Vöhringer, and V.A. Lubarda. "The Onset of Twinning in Metals: A Constitutive Description." *Acta Metallurgica et Materialia*. Vol. 49. pp. 4,025-4,039. 2001.

Miller, W.H., R.T. Chen, and E.A. Starke, Jr. "Microstructure, Creep, and Tensile Deformation in Ti-6Al-2Nb-1Ta-0.8Mo." *Metallurgical Transactions A*. Vol. 18A. pp. 1,451-1,468. 1987.

Neeraj, T., D.-H. Hou, G.S. Daehn, and M.J. Mills. "Phenomenological and Microstructural Analysis of Room Temperature Creep in Titanium Alloys." *Acta Metallurgica et Materialia*. Vol. 48. pp. 1,225-1,238. 2000.

Oberson, P.G. and S. Ankem. "Why Twins Do Not Grow at the Speed of Sound all the Time." *Physical Review Letters*. Vol. 95. pp. 165501/1-4. 2005.

Odegard, B.C. and A.W. Thompson. "Low Temperature Creep of Ti-6Al-4V." *Metallurgical Transactions*. Vol. 5. pp. 1,207-1,213. 1974.

Partridge, P.G. "The Crystallography and Deformation Modes of Hexagonal Close-Packed Metals." *Metallurgical Reviews*. Vol. 118. pp. 169-193. 1968.

Paton, N.E., J.C. Williams, and G.P. Rauscher. "The Deformation of α -Phase Titanium." *Titanium Science and Technology*. R.I. Jaffee and H.M. Burte, eds. New York City, New York: Plenum Press. pp. 1,049-1,069. 1973.

Peters, M. and G. Luetjering. "Control of the Microstructure and Texture in Ti-6Al-4V Alloy." Proceedings of the 4th International Conference on Titanium. *Titanium '80 Science and Technology*. H. Kimura and O. Izumi, eds. Warrendale, Pennsylvania: TMS-AIME. pp. 925-935. 1980.

Riemann, W.H. "Room Temperature Creep in Ti-6Al-4V." *Journal of Materials, JMLSA*. Vol. 6. pp. 926-940. 1971.

Shelton, C.G. and B. Ralph. "The Deformation of Two Phase Ti-6Al-4V." Proceedings of the 4th Risø International Symposium on Metallurgy and Materials Science. *Deformation of Multi-Phase and Particle Containing Materials*. J.B. Bilde-Sorensen, N. Hansen, A. Horsewell, T. Leffers, and H. Liholt, eds. Roskilde, Denmark: Risø National Laboratory. pp. 531–538. 1983.

Song, S.G. and G.T. Gray, III. "Influence of Temperature and Strain rate on Slip and Twinning Behavior of Zr." *Metallurgical and Materials Transactions A*. Vol. 26A. pp. 2,665–2,675. 1995a.

———. "Structural Interpretation of the Nucleation and Growth of Deformation Twins in Zr and Ti–I. Application of the Coincident Site Lattice (CSL) Theory to Twinning Problems in H.C.P. Structures." *Acta Metallurgica et Materialia*. Vol. 43. pp. 2,325–2,337. 1995b.

Suri, S., G.B. Viswanathan, T. Neeraj, D.-H. Hou, and M.J. Mills. "Room Temperature Deformation and Mechanisms of Slip Transmission in Oriented Single-Colony Crystals of an α / β Titanium Alloy." *Acta Metallurgica et Materialia*. Vol. 47. pp. 1,019–1,034. 1999.

Thompson, A.W. and B.C. Odegard. "The Influence of Microstructure on Low Temperature Creep of Ti-5Al-2.5Sn." *Metallurgical Transactions*. Vol. 4. pp. 899–908. 1973.

Tung, P.P. and A.W. Sommer. "Dislocation Energetics in Alpha Titanium." *Metallurgical Transactions*. Vol. 1. pp. 947–953. 1970.

Wanjara, P. and M. Jahazi. "Linear Friction Welding of Ti-6Al-4V: Processing, Microstructure, and Mechanical-Property Inter-Relationships." *Metallurgical and Materials Transactions A*. Vol. 36A. pp. 2,149–2,164. 2005.

Williams, D.B. and C.B. Carter. *Transmission Electron Microscopy: A Textbook for Materials Science*. New York City, New York: Plenum Press. 1996.

Yoo, M.H. "Slip, Twinning, and Fracture in Hexagonal Close-Packed Metals." *Metallurgical Transactions A*. Vol. 12A. pp. 409–418. 1981.

Zeyfang, R.R., R. Martin, and H. Conrad. "Low Temperature Creep of Titanium." *Materials Science and Engineering*. Vol. 8. pp. 134–140. 1971.

APPENDIX A

TENSILE DATA

Tensile tests were performed for Titanium Grade 7 and Grade 5 to determine the 0.2 percent yield stress to perform the creep tests at a known percentage of the yield stress.

A.1 Titanium Grade 7

A.1.1 Experimental Procedure

Tensile tests for Titanium Grade 7 were performed at the temperatures of 25, 50, 100, and 150 °C [77, 122, 212, and 302 °F]. The strain rate was 0.005 per minute up to 0.4 percent strain and then 0.05 per minute until rupture.

A.1.2 Results and Discussion

Tensile curves at the respective temperatures are shown on Figure A–1. The 0.2 percent yield stress decreases with an increase in temperature (refer to Figure A–2), and it can be approximated as a linear function of temperature.

The notable feature of the stress–strain curves shown in Figure A–1 is the decrease in stress, or load drop, after yielding at 100 and 150 °C [212 and 302 °F]. This behavior is unusual, because in most metals and alloys, the stress level required for further deformation stays constant or increases after yielding. When the stress increases after yielding, the phenomenon is known as strain hardening. Strain hardening is usually caused by the increase in dislocation density during plastic deformation. The dislocations become tangled, and it is more difficult for them to move. As such, increased stress is required to produce more plastic strain.

The load drop phenomenon after yielding has been previously observed for α -titanium alloys (Orava, et al., 1966; Jones and Conrad, 1969). Orava, et al. (1966) have recorded such a load drop in A-70 titanium (commercially pure titanium with an additional 0.27 weight percent of oxygen) wire, with the greatest load drop between 77 and 177 °C [171 and 351 °F]. This temperature range is consistent with the load drop temperatures recorded in the present study for Titanium Grade 7. Jones and Conrad (1969) measured the dislocation density in A-70 titanium before testing at the initial peak point of the stress–strain curve (the maximum point before the load drop), during the load drop (halfway between the maximum and the minimum), and at the minimum point of the stress-strain curve (after the load drop and before any rehardening). Initially, or before testing, they found relatively few randomly distributed dislocations. At the initial peak point, there were discrete narrow bands of dislocations in about half of the grains. During the load drop, the dislocation density increased significantly, mainly by the number of slip bands in some of the grains. Finally, at the minimum point, the dislocation density had increased further and almost all the grains contained dislocations. Straining beyond this point required additional stress, indicative of conventional strain hardening. Thus, the load drop could be attributed to an increase in the density of mobile dislocations. Also, this type of behavior has been observed by Vijayshankar and Ankem (1990) for β -titanium alloys at high temperature.

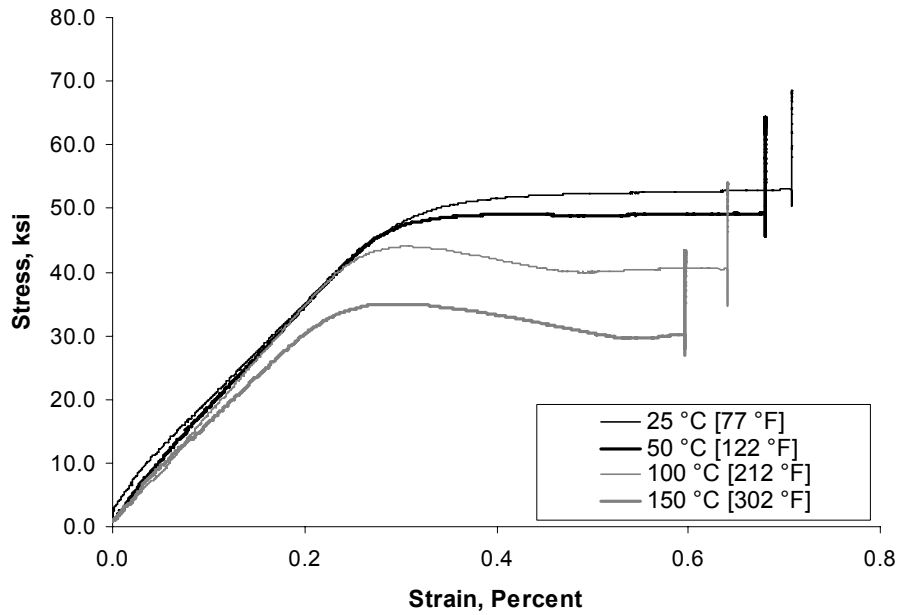


**Figure A-1. Tensile Curves for Titanium Grade 7 at Various Temperatures
{Units: ksi [1 ksi = 6.895 MPa]}**

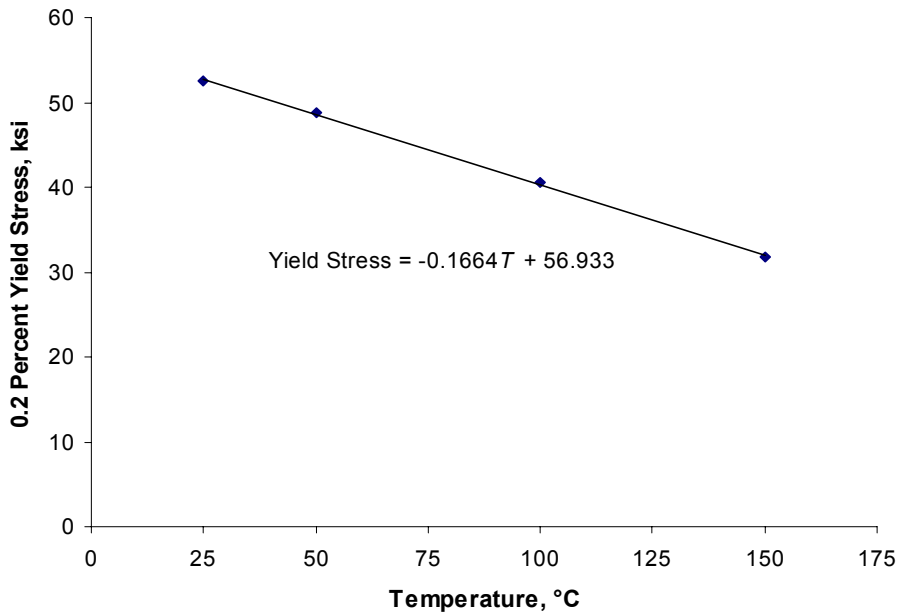


Figure A-2. The 0.2 Percent Yield Stress as a Function of Temperature Along With the Fitting Empirical Equation for Titanium Grade 7

The increase in mobile dislocation density in Titanium Grade 7 at 100 and 150 °C [212 and 302 °F] can explain the load drop after the initial maximum yield point. At this elevated temperature, dislocations, which may be pinned by interstitial oxygen atoms, can become unpinned and free to glide and contribute to plastic deformation. This load drop will not occur at the lower temperatures 25 and 50 °C [77 and 122 °F], because dislocations cannot become unpinned from interstitial oxygen atoms and additional stress is needed to create more mobile dislocations for plastic deformation to continue. This suggestion is consistent with the Conrad and Jones (1970) observation that in commercially pure iodide titanium, which has very little oxygen content (0.003 weight percent of oxygen), there is no load drop.

A.2 Titanium Grade 5

A.2.1 Experimental Procedure

Tensile tests for Titanium Grade 5 (Ti-6Al-4V) were performed at the temperatures of 25, 100, 150, and 250 °C [77, 212, 302, and 482 °F]. The strain rate was 0.005 per minute up to 0.4 percent strain and then 0.05 per minute until rupture.

A.2.2 Results and Discussion

Tensile curves at the respective temperatures are shown in Figure A–3. The 0.2 percent yield stress decreases with an increase in temperature. A plot of 0.2 percent yield stress as a function of temperature (refer to Figure A–4) indicates that the 0.2 percent yield stress decreases with temperature, and it can be approximated as a linear-type behavior. These results are consistent with previous results for Ti-6Al-4V with similar chemical composition, microstructure, and texture (Boyer, 1994; U.S. Department of Defense, 1998).

The notable feature of the stress–strain curves shown on Figure A–3 for the specimen tested at 250 °C [482 °F] is an increase in stress required for further strain after yielding, or work hardening. The specimens tested at the lower temperatures showed no work hardening. In a previous investigation of Ti-6Al-4V; Follansbee and Gray (1989), found that during deformation above 200°C [392 °F], the dislocation morphology was more random and tangled than below 200°C [392 °F], contributing to increased work hardening at elevated temperatures.

A.3 References

Boyer, R., G. Welsch, and E.W. Collings, eds. *Materials Properties Handbook: Titanium Alloys*. Materials Park, Ohio: ASM International. 1994.

Conrad, H. and R.L. Jones. “Effects of Interstitial Content and Grain Size on the Mechanical Behavior of Alpha Titanium Below $0.4 T_m$.” *The Science, Technology and Application of Titanium*. R.I. Jaffee and N.E. Promise, eds. Oxford, United Kingdom: Pergamon Press. pp. 491–501. 1970.

Follansbee, P.S. and G.T. Gray, III. “An Analysis of the Low Temperature, Low and High Strain-Rate Deformation of Ti-6Al-4V.” *Metallurgical Transactions A*. Vol. 20A. pp. 863–874. 1989.

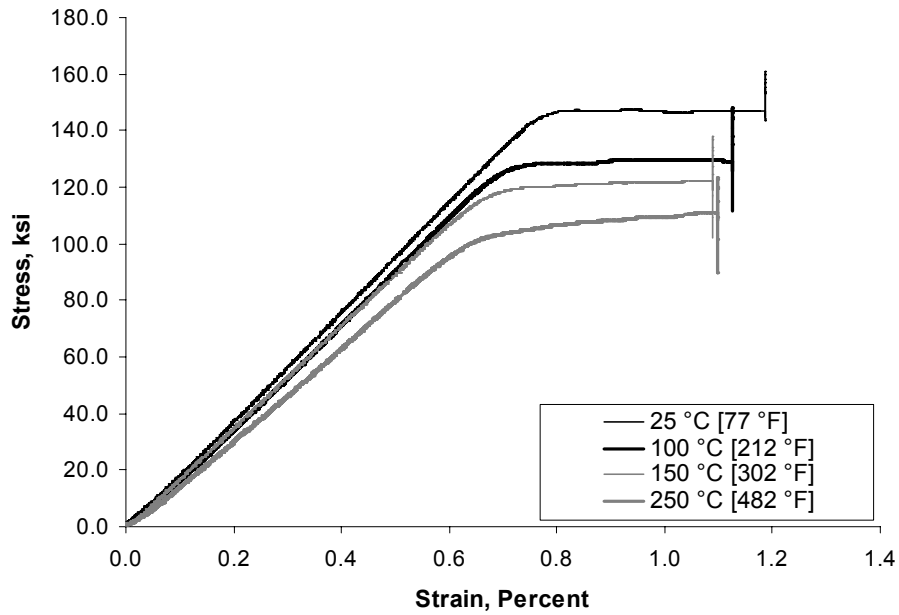


Figure A-3. Tensile Curves for Titanium Grade 5 at Various Temperatures (Units: ksi [1 ksi = 6.895 MPa])

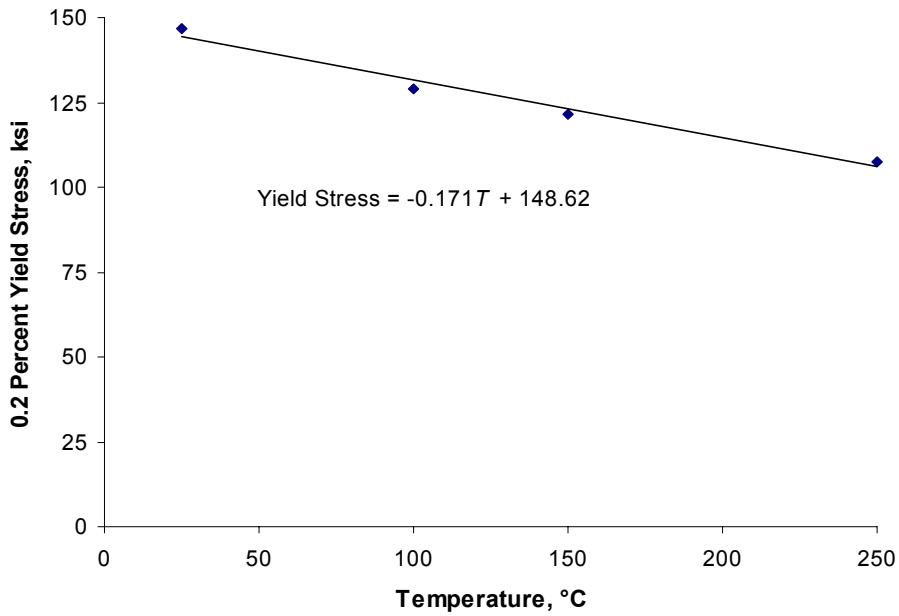


Figure A-4. The 0.2 Percent Yield Stress as a Function of Temperature Along With the Fitting Empirical Equation for Titanium Grade 5

Jones, R.L. and H. Conrad. "The Effect of Grain Size on the Strength of Alpha-Titanium at Room Temperature." *Transactions of the Metallurgical Society of AIME*. Vol. 245. pp. 779–789. 1969.

Orava, R., G. Stone, and H. Conrad. "Effects of Temperature and Strain Rate on Yield and Flow Stresses of Alpha-Titanium." *Transactions ASM*. Vol. 58. pp. 171–184. 1966.

U.S. Department of Defense. *Military Handbook: Metallic Materials and Elements for Aerospace Vehicle Structures*. MIL–DBK–5H. Washington, DC: U.S. Department of Defense. 1998.

Vijayshankar, M.N. and S. Ankem. "High Temperature Tensile Deformation Behavior of β -Titanium." *Materials Science and Engineering A*. Vol. 129. pp. 229–237. 1990.

APPENDIX B

TEXTURE ANALYSIS

The texture of a polycrystalline material such as Titanium Grade 7 and Grade 5 will affect the operative deformation mechanisms and mechanical properties of the material. The texture of as-received (rolled) Titanium Grade 7 and Grade 5 were determined by x-ray diffraction techniques.

B.1 Titanium Grade 7

Titanium Grade 7, which is α -titanium, has the hexagonal close-packed crystal structure. The hexagonal close-packed system is most easily visualized by considering three unit cells arranged together to form one large cell, as shown in Figure B-1. For this large cell, Figure B-2 illustrates important crystallographic planes and directions in the hexagonal close-packed system (Oberson, 2006). Titanium Grade 7 is polycrystalline material, (i.e., the bulk material is made up of many small crystals, or grains). Each crystal or grain is made up of millions or billions of unit cells that have the same crystallographic orientation. Each grain in the polycrystalline material has its own respective orientation and its size is usually on the scale of microns. Also, the size and morphology of the grains are dependent on the thermo-mechanical processing of the material.

A metal that has undergone severe deformation, as in rolling, will develop a preferred orientation or texture in which certain crystallographic planes tend to orient themselves in a preferred manner with respect to the direction of maximum strain. Essentially, texture is the distribution of crystallographic orientations of a sample. A sample in which the crystallographic orientation is random has no texture. If the crystallographic orientation is not random, as after rolling, the sample has texture. In the case of a single crystal, the slip planes tend to rotate parallel to the axis of principal strain. The same tendency exists in a polycrystalline material, but the individual grains cannot rotate freely; therefore, the analysis is more complex. Various textures are schematically illustrated in Figure B-3.

B.1.1 Pole Figures

The texture of a polycrystalline material is typically characterized by using x-ray diffraction to determine which crystallographic planes are parallel to the surface of the material. The x-ray pattern of a polycrystalline metal will show points corresponding to different planes where the angles satisfy the condition for Bragg reflection (Bragg, 1914). If the grains are randomly oriented, the distribution of the spots will be uniform (random). If, however, the material shows texture, there will be dense arrays of points in various locations. These dense areas indicate the orientation of the poles (normals) of a particular crystallographic plane. The orientation of the grains of a particular crystallographic orientation with respect to the rolling and transverse directions is typically illustrated by means of a pole figure.

A pole figure is a stereographic projection of the crystallographic directions present in the grains that constitute a material. For the representation of texture in rolled materials on pole figures, the axes of the projection sphere are aligned with the axes of the sample. The sample normal is the center of the projection and the rolling direction (RD) chosen to be on the right or at the top of the projection, as schematically illustrated in Figure B-4. A pole figure of the type shown in Figure B-5 will result.

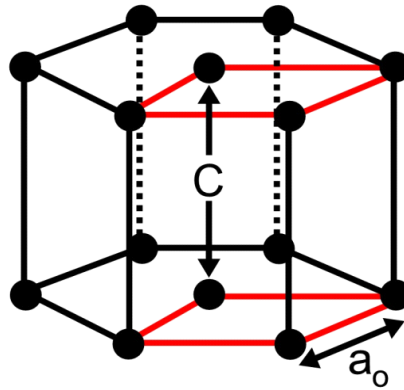


Figure B-1. A Point Model of the Hexagonal Close-Packed Unit Cell of α -Titanium Showing the Relationship Between the Smaller Primitive Unit Cell (Outlined in Red) and the More Convenient Large Unit Cell

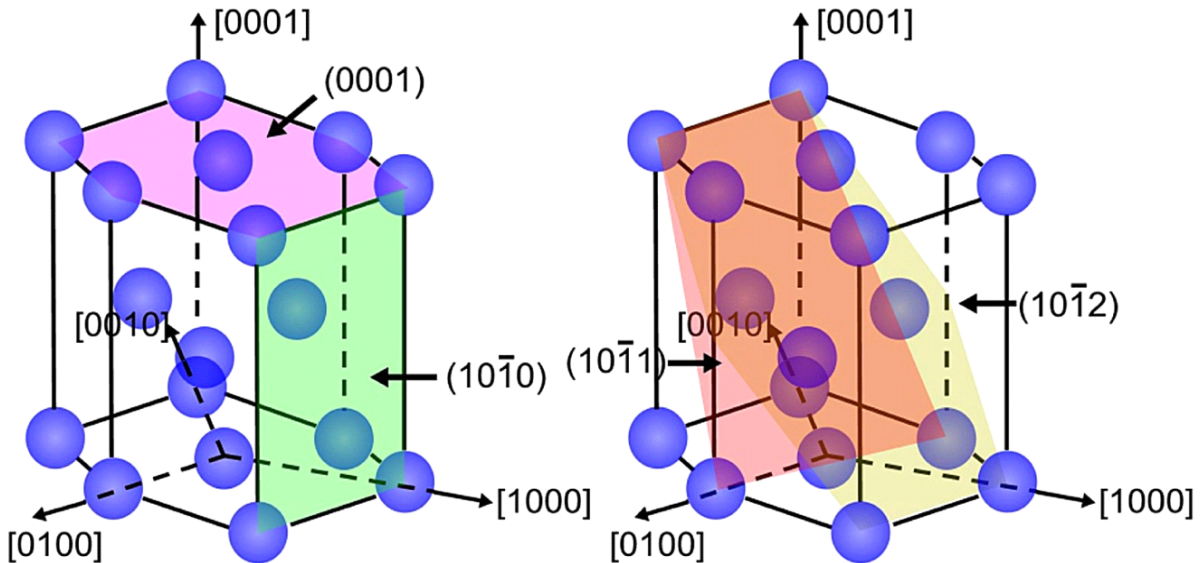


Figure B-2. Schematic of the Hexagonal Close-Packed Unit Cell of α -Titanium Illustrating Various Important Planes and Directions (Oberson, 2006)

B.1.2 Inverse Pole Figures

A standard pole figure gives the orientation distribution of a particular crystallographic plane with respect to the reference directions (rolling and transverse). While this is useful, it is often more convenient to describe texture using the inverse pole figure. The inverse pole figure gives the orientation of the reference axis with respect to the standard crystallographic directions. In

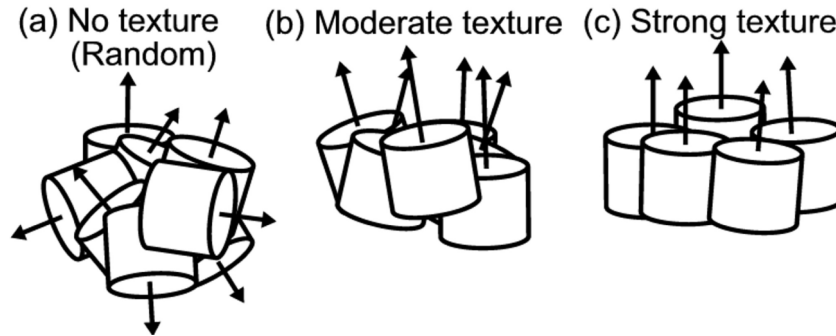


Figure B-3. Schematic Illustration of a Polycrystal With (a) No texture (Random), (b) Moderate Texture, and (c) Strong Texture

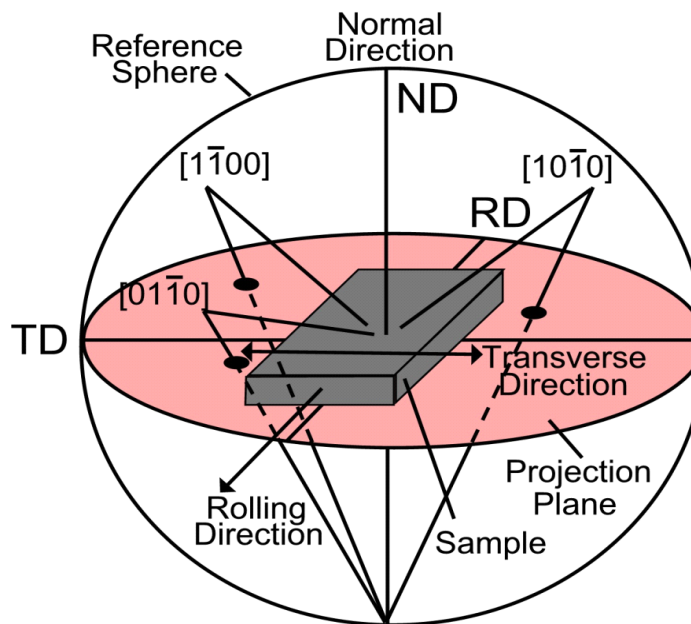


Figure B-4. Schematic Illustration of Generating a Pole Figure. The Rolling Plate Normal Direction (ND) Is the Center of the Projection and the Rolling Direction (RD) Is Chosen To Be on the Right or at The Top of the Projection.

other words, the inverse pole figure gives the distribution of crystallographic directions parallel to certain sample directions (Jetter, et al., 1956). Consider a polycrystalline material with a predominant texture as shown in Figure B-6(a), where the $[0001]$ direction is parallel to the normal direction (ND). For a particular specimen, three inverse pole figures describe the texture: one each for the normal, rolling, and transverse directions. In an inverse pole figure, each of the three corners of the “wedge” corresponds to the indicated crystallographic direction. A high density of points at the corner indicates that for the given direction (e.g., the normal

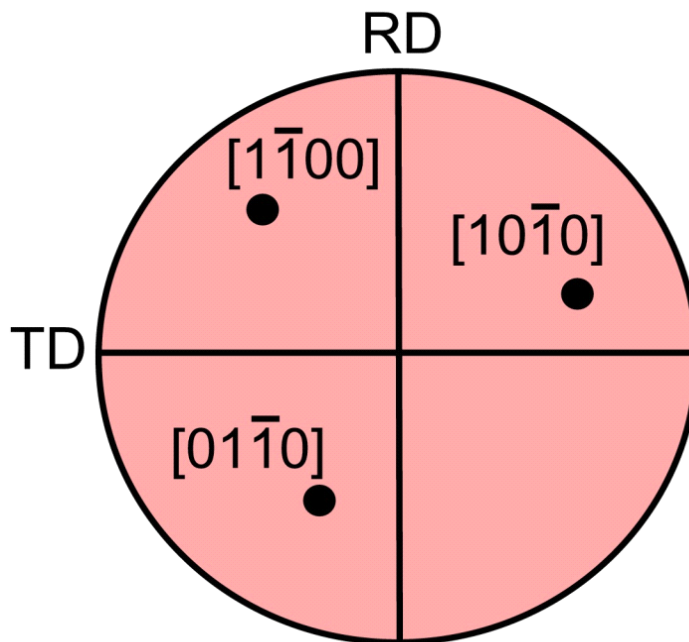


Figure B-5. Pole Figure as Generated from the Example Shown in Figure B-4

direction) a large number of poles in the specimen are oriented in the direction that corresponds to that corner.

The inverse pole figure for the normal direction (ND) of the crystal shown in Figure B-6(a), as given in Figure B-6(b), shows a high density of poles oriented in the $[0001]$ direction. Similar inverse pole figures can be generated for the rolling and transverse directions to show the pole density in these directions.

B.1.3 Results and Discussion

For Titanium Grade 7, five pole figures were prepared where the normal directions are $[0002]$, $\langle 1\bar{1}00 \rangle$, $\langle 10\bar{1}1 \rangle$, $\langle 10\bar{1}2 \rangle$, and $\langle 11\bar{2}0 \rangle$. These pole figures are shown in Figure B-7.

Additionally, inverse pole figures were prepared for the normal, rolling, and transverse directions, as shown in Figure B-8. The pole figures and inverse pole figures show that as-received Titanium Grade 7 has the following texture:

- Strong basal $[0001]$ texture in the normal direction
- Strong prism $\langle 1\bar{1}00 \rangle$ texture in the rolling direction
- Moderate basal and pyramidal $\langle 1\bar{1}01 \rangle$ texture in the transverse direction

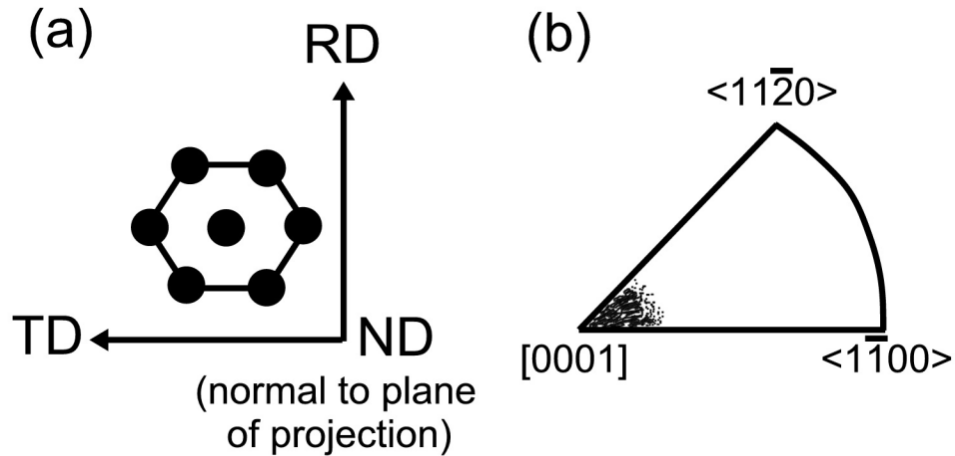


Figure B-6. (a) Schematic Illustration of a Hexagonally Close-Packed Unit Cell in Which the $[0001]$ Direction Is Parallel to the Normal Direction (ND). (b) Inverse Pole Figure for a Polycrystalline Material Whose Texture is Predominantly Shown in (a). There Is a High Density of Poles in the $[0001]$ Corner.

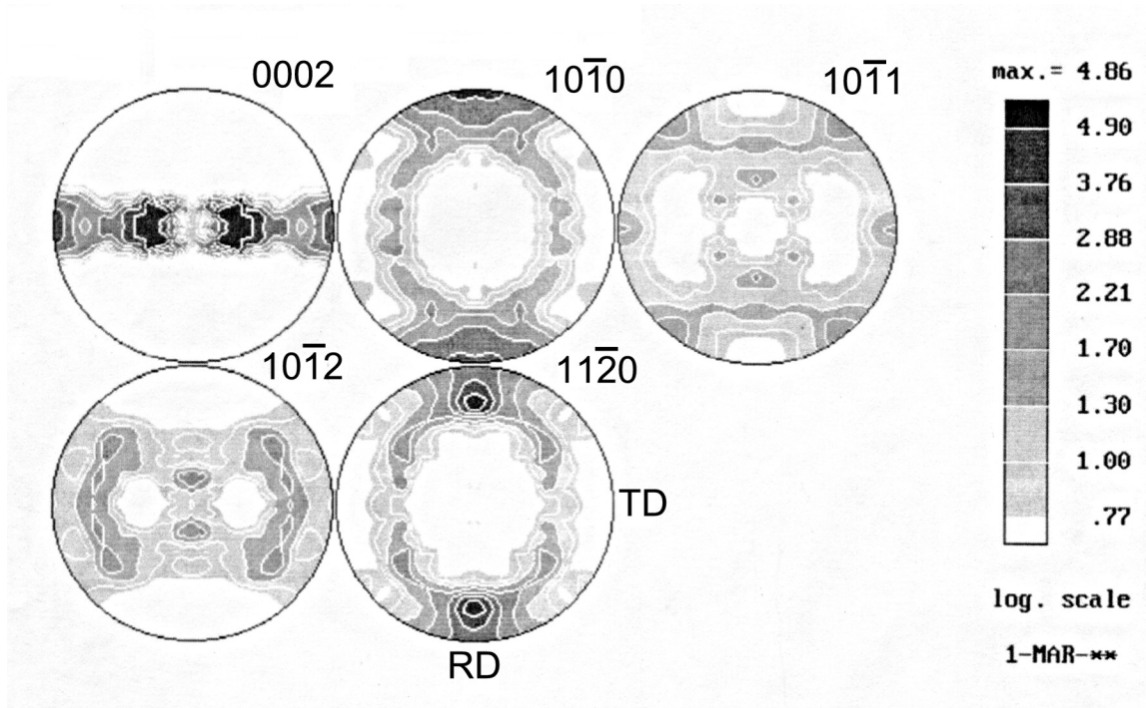


Figure B-7. Pole Figures for As-Received Titanium Grade 7. The Normal Direction Is Given at the Upper Right of the Pole Figure. The Rolling Direction (RD) Is Vertical and the Transverse Direction (TD) Is Horizontal. Darker Areas Indicate Areas of Higher Pole Density.

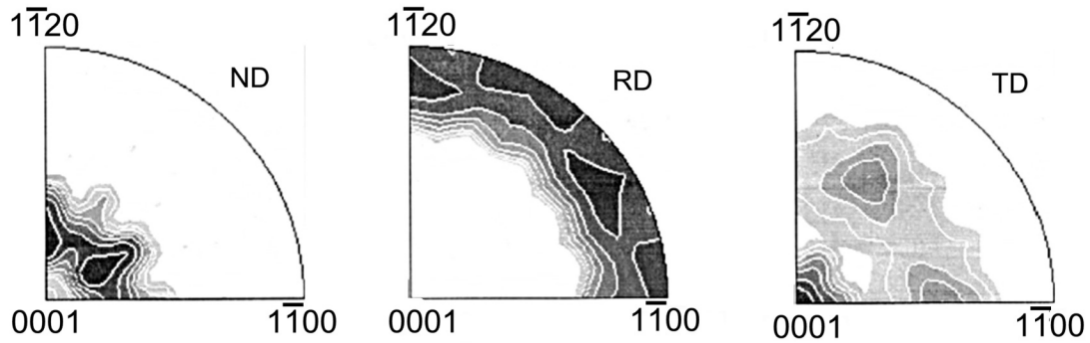


Figure B-8. Inverse Pole Figures for As-Received Titanium Grade 7 for the Normal Direction (ND), Rolling Direction (RD), and Transverse Direction (TD). The Corners of the Inverse Pole Figure Correspond to the Indicated Crystallographic Direction.

This type of texture is typical for cold-rolled α -titanium (Inagaki, 1991) and is schematically illustrated in Figure B-9. It is often convenient to describe texture by the indices $\{hkil\}\langle uvw \rangle$, where $\{hkil\}$ refers to the family of crystallographic planes parallel to the surface of the sample and $\langle uvw \rangle$ corresponds to the family of crystallographic directions parallel to the rolling direction. In this case, the texture can be given as $\{\bar{2}115\}\langle 1\bar{1}00 \rangle$.

As previously mentioned, the texture of the material will have a significant effect on the operative deformation mechanisms and on the mechanical properties overall. Other investigators (Mullins and Patchett, 1981; Murayama, et al., 1993) have studied the tensile properties of cold-rolled, commercially-pure titanium alloys when loaded along different stress axes (i.e., the loading axis is either parallel to the rolling direction or the transverse direction). When loaded in the transverse direction, as in this investigation for Titanium Grade 7, the predominant slip system was found to be $\langle 11\bar{2}0 \rangle\{1\bar{1}00\}$, which is referred to as *a*-type prism slip. Moreover, the predominant twinning system activated in this loading orientation is one that is activated by *c*-axis tension—namely, the $\{1\bar{1}02\}$ twinning system. As such, *a*-type prism slip and $\{1\bar{1}02\}$ twinning should be the predominant deformation mechanisms in the Titanium Grade 7.

B.2 Titanium Grade 5

The texture of Titanium Grade 5 is more complex to describe than that of Titanium Grade 7 because Titanium Grade 5 is a two-phase alloy. A two-phase alloy is an alloy in which there is a mixture of regions with different crystal structures. In the case of the two-phase α - β Ti-6Al-4V alloy, such as Titanium Grade 5, there are regions that have the hexagonal close-packed crystal structure α , like that found in Titanium Grade 7, and regions that have

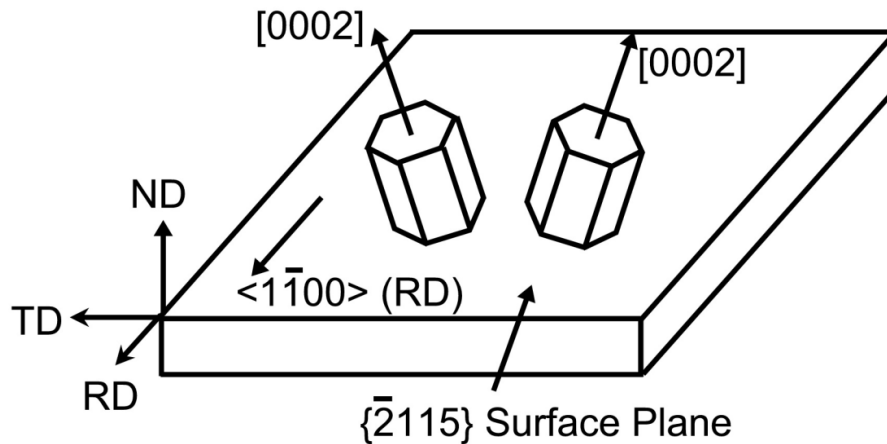


Figure B-9. Schematic Illustration of $\{2115\}\langle 1\bar{1}00 \rangle$ Texture in As-Received Titanium Grade 7

the body-centered cubic crystal structure β . Thus, the texture must be described for both phases, as this will affect the mechanical properties of the two-phase alloy.

B.2.1 Crystal Structures in the Two-Phase Titanium Grade 5

The crystal structure of the hexagonal close-packed phase α of the two-phase $\alpha - \beta$ Ti-6Al-4V alloy was described in Section B.1. The crystal structure of the β -phase is known as the body-centered cubic. This structure can be described as a cube defined by eight atoms with an additional atom in the center of the cube. Some important directions and planes in this structure are illustrated in Figure B-10 (Oberson, 2006).

B.2.2 Orientation Relationship Between the α and β Phases

While the respective phases of the two-phase $\alpha - \beta$ Titanium alloy have different crystal structures, there is a relationship between the two phases in terms of how they are oriented with respect to one another. The two phases have a Burgers orientation relationship (Newkirk and Geisler, 1953). This means that a particular crystallographic direction or plane in the α -phase particle grain is aligned with (is parallel to) a particular crystallographic direction or plane in the adjacent β -phase particle grain. For $\alpha - \beta$ Titanium alloys, such as Titanium Grade 5, the Burgers orientation relationship is given by $(0001)_{\alpha} \parallel \{110\}_{\beta}$ and $\langle 11\bar{2}0 \rangle_{\alpha} \parallel \langle 111 \rangle_{\beta}$. It is suggested that this Burgers orientation relationship allows for the easy transmission of slip across the interphase interface (Miller, et al., 1987). The need to maintain a coherent interphase interface during deformation of the two-phase alloy leads to elastic interaction stresses.

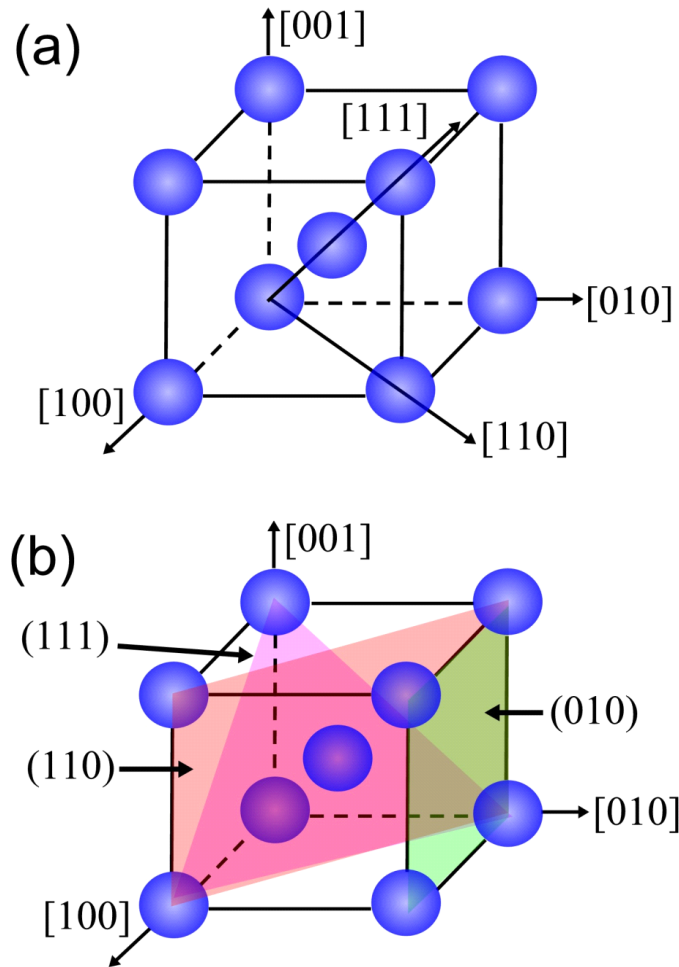


Figure B–10. Schematic Illustration of the Body-Centered Cubic Crystal Structure, as Found in the β -Phase of Titanium Grade 5, Showing Important Crystallographic Directions in (a) and Crystallographic Planes in (b) (Oberson, 2006)

B.2.3 Elastic Interaction Stresses

Elastic interaction stresses arise due to differences in the elastic properties of two ductile phases that are constrained at the interface (Ankem and Margolin, 1986). A well defined interface between the phases constrains the α and β phases, such that the strain in each phase at the interface must be equal. In the case of the two-phase titanium alloy, the yield strength of the α phase is lower than that of the β phase, and the elastic modulus of the β phase is lower than that of the α phase. Thus, at a given applied stress on the two-phase alloy, the stress and strain of the α phase will be increased in excess of the applied stress level, while the stress on the β phase will be decreased to maintain an equivalent strain on each phase at the interface. Therefore, the α phase in the two-phase alloy can deform

plastically at applied stress levels that would normally result only in elastic deformation in a single-phase alloy.

B.2.4 Results and Discussion

For Titanium Grade 5, pole figures were prepared for the α and β -phases of the two-phase alloy. For the α -phase the normal directions are $[0002]$, $\langle 1\bar{1}00 \rangle$, $\langle 1\bar{1}01 \rangle$, $\langle 1\bar{1}02 \rangle$, and $\langle 11\bar{2}0 \rangle$. For the β -phase, the normal directions are $\langle 110 \rangle$, $\langle 200 \rangle$, and $\langle 211 \rangle$. The pole figures for the α -phase and β -phase are shown in Figures B–11 and B–12, respectively. Additionally, inverse pole figures were prepared for the normal, rolling, and transverse directions of both phases, as shown in Figures B–13 and B–14.

The pole figures and inverse pole figures indicate the following texture for the as-received Titanium Grade 5. For the α -phase

- Prism $\langle 11\bar{2}0 \rangle$ texture in the normal direction
- Strong basal $[0001]$ texture in the transverse direction
- Moderate prism $\langle 1\bar{1}00 \rangle$ texture in the rolling direction

For the β -phase

- $\langle 100 \rangle$ and $\langle 111 \rangle$ texture in the normal direction
- Strong $\langle 110 \rangle$ texture in the transverse direction
- Little texture in the rolling direction

This texture is similar to that observed in previous investigations of the cold-rolled texture of α - β Ti-6Al-4V (Frederick and Lenning, 1975; Gu and Hardie, 1997). Moreover, the texture is consistent with the Burgers orientation relationships given earlier. In particular, note that for the transverse direction, $[0001]_{\alpha}$ is aligned with $\langle 110 \rangle_{\beta}$, and for the normal direction, $\langle 11\bar{2}0 \rangle_{\alpha}$ is aligned with $\langle 111 \rangle_{\beta}$. The fact that the Burgers orientation relationship is obeyed makes it likely that slip will be able to cross the α - β interface.

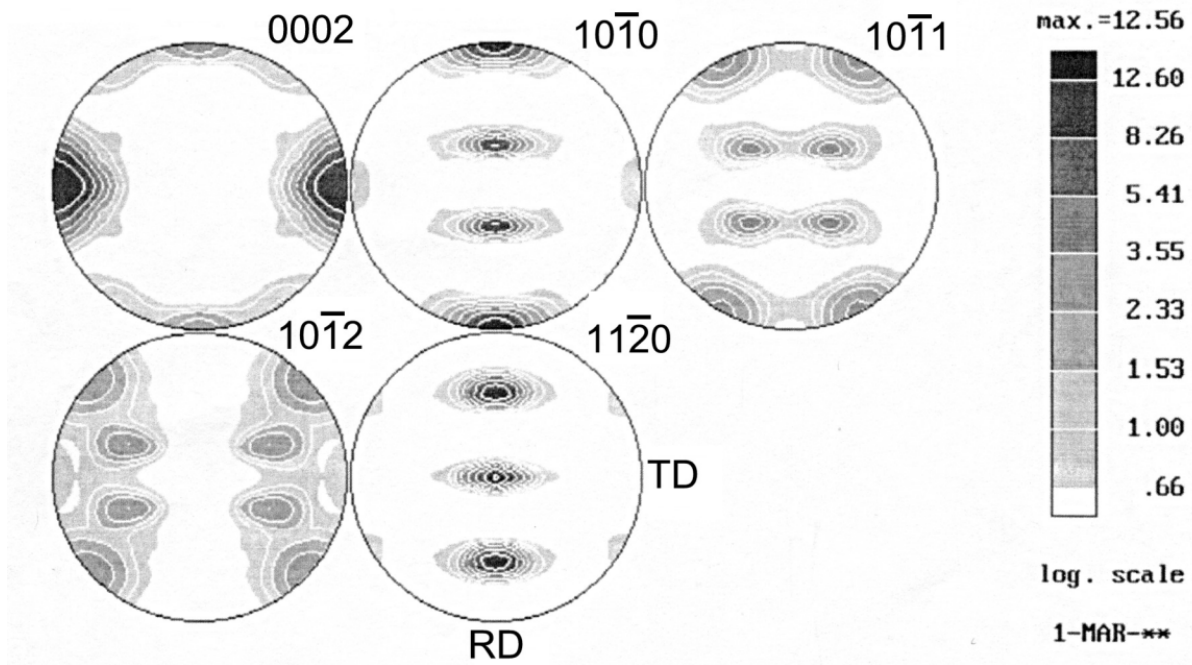


Figure B-11. Pole Figures for the α -Phase of As-Received Titanium Grade 5. The Normal Direction Is Given at the Upper-Right of the Pole Figure. The Rolling Direction (RD) is Vertical and the Transverse Direction (TD) Is Horizontal. Darker Areas Indicate Higher Pole Density.

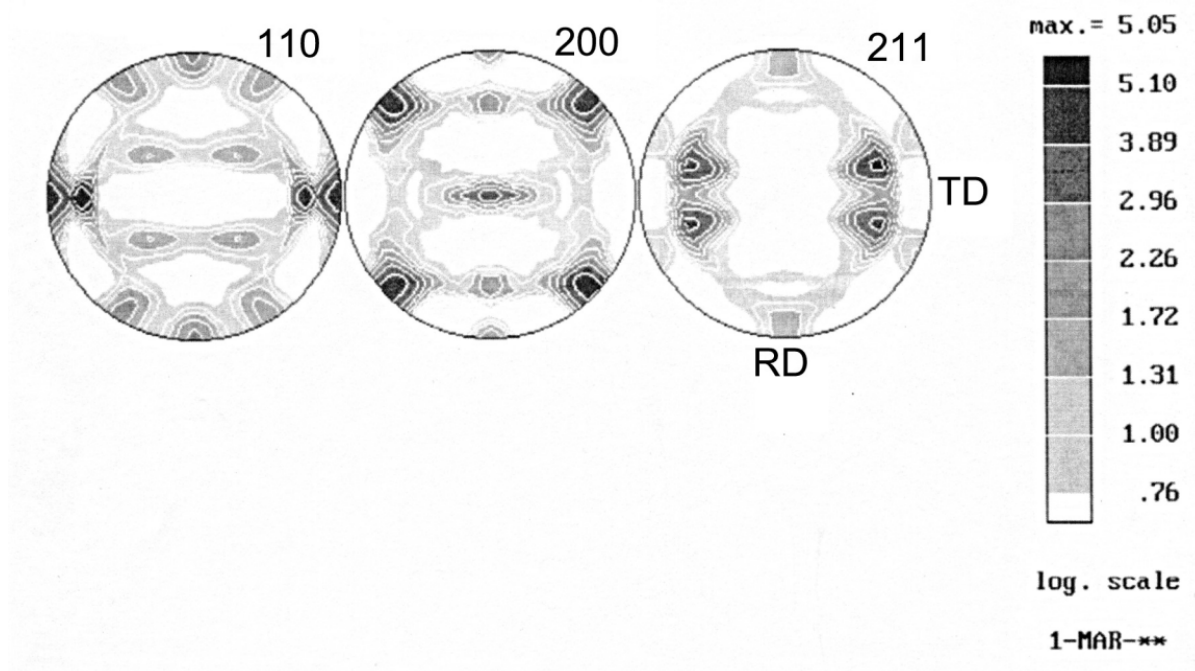


Figure B-12. Pole Figures for the β -Phase of As-Received Titanium Grade 5. The Normal Direction Is Given at the Upper Right of the Pole Figure. The Rolling Direction (RD) Is Vertical and the Transverse Direction (TD) Is Horizontal. Darker Areas Indicate Higher Pole Density.

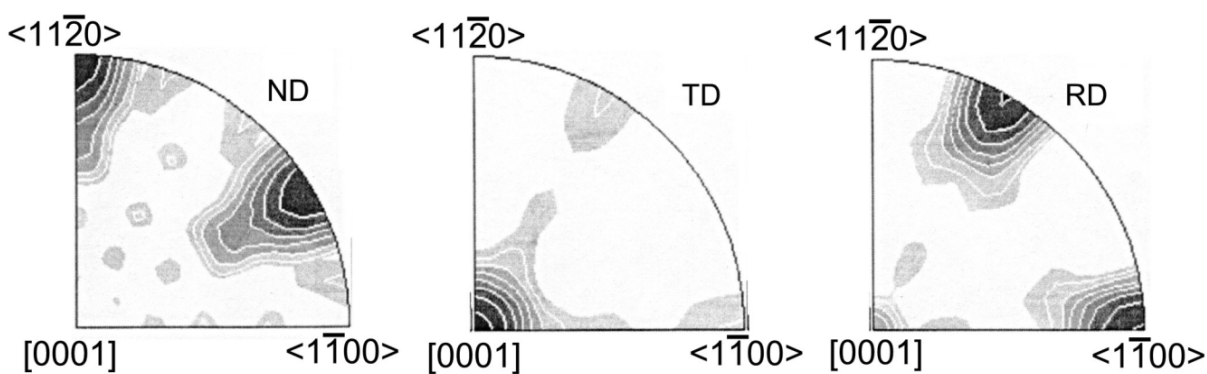


Figure B-13. Inverse Pole Figures for the α -Phase of As-Received Titanium Grade 5 for the Normal Direction (ND), Rolling Direction (RD), and Transverse Direction (TD). The Corners of the Inverse Pole Figure Correspond to the Indicated Crystallographic Direction.

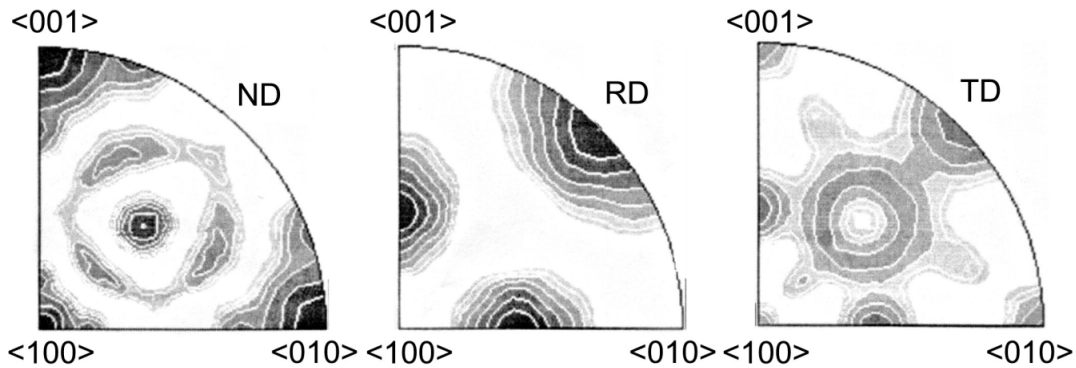


Figure B-14. Inverse Pole Figures for the β -Phase of As-Received Titanium Grade 5 for the Normal Direction (ND), Rolling Direction (RD), and Transverse Direction (TD). The Corners of the Inverse Pole Figure Correspond to the Indicated Crystallographic Direction.

B.3 References

Ankem, S. and H. Margolin. "A Rationalization of Stress-Strain Behavior of Two-Ductile Phase Alloys." *Metallurgical Transactions A*. Vol. 17A. pp. 2,209–2,226. 1986.

Bragg, W.L. "The Diffraction of Short Electromagnetic Waves by a Crystal." *Proceedings of the Cambridge Philosophical Society*. Vol. 17. pp. 43–57. 1914.

DOE. DOE/RW-0508, "Viability Assessment of a Repository at Yucca Mountain." Overview and all five volumes. Las Vegas, Nevada: DOE, Office of Civilian Radioactive Waste Management. 1998.

Frederick, S.F. and G.A. Lenning. "The Influence of Prior Texture on the Cold Rolled Texture of Ti-6Al-4V." *Metallurgical Transactions A*. Vol. 6A. pp. 1,467–1,468. 1975.

Gu, J. and D. Hardie. "The Effect of Hydrogen on the Tensile Ductility of Ti6Al4V." *Journal of Materials Science*. Vol. 32. pp. 603–608. 1997.

Inagaki, H. "Development of Cold-Rolling Textures in Pure Ti." *Zeitschrift fur Metallkunde*. Vol. 82. pp. 779–789. 1991.

Jetter, L.K., C.J. McHarguhe, and R.O. Williams. "Method of Representing Preferred Orientation Data." *Journal of Applied Physics*. Vol. 27. pp. 368–374. 1956.

Miller, W.H., R.T. Chen, and E.A. Starke, Jr. "Microstructure, Creep, and Tensile Deformation in Ti-6Al-2Nb-1Ta-0.8Mo." *Metallurgical Transactions A*. Vol. 18A. pp. 1,451–1,468. 1987.

Mullins, S. and B.M. Patchett. "Deformation Microstructures in Titanium Sheet Metal." *Metallurgical Transactions A*. Vol. 12A. pp. 853–863. 1981.

Murayama, Y., K. Obara, and K. Ikeda. "Effect of Twinning on Deformation of Textured Commercially-Pure Ti Sheets under Plane Stress States." *Materials Transactions, JIM*. Vol. 34. pp. 801–808. 1993.

Newkirk, J.B. and A.H. Geisler. "Crystallographic Aspects of the Beta to Alpha Transformation in Titanium." *Acta Metallurgica*. Vol. 1. pp. 370–374. 1953.

Oberson, P.G. "An Experimental and Theoretical Investigation of the Low Temperature Creep Deformation Mechanisms of Single Phase Titanium Alloys." Ph.D. dissertation. University of Maryland. College Park, Maryland. 2006.

APPENDIX C

LOW TEMPERATURE TENSILE AND CREEP TESTS OF TITANIUM GRADE 7 AND GRADE 5

C.1 Tensile Test Results

Westmoreland Mechanical Testing and Research, Inc. conducted tensile tests of both Titanium Grade 7 and Grade 5 at four temperatures—25, 100, 150, and 250 °C [77, 212, 302, and 72 °F]. Moreover, an additional tensile test for Titanium Grade 7 was performed at 50 °C [122 °F]. The room temperature {25 °C [77 °F]} test was conducted in accordance with ASTM E-8 specification (ASTM International, 2007a). Elevated temperature tensile tests were performed in accordance with ASTM E-21 specification (ASTM International, 2007b). For each temperature, two specimens were tested. The tensile test results, including ultimate tensile strength, 0.2 percent yield stress, percent elongation, percent reduction in area, and modulus of elasticity for Titanium Grade 7 and Grade 5 are reported in Tables C–1, and C–2, respectively.

C.2 Creep Test Results

Creep deformation tests were conducted for several different scenarios based on previous studies, such as the investigation of fundamental mechanical properties of Alloy 22 performed by Dunn, et al. (2005). The general factors that affect creep deformation are the stress levels, temperature, loading time, and microstructure of the material. Therefore, a matrix of loading conditions covering the parameter combinations at the emplacement level was generated. The parameter ranges considered in the tests for samples of Titanium Grade 7 and Grade 5 are as follows:

- Creep tests were conducted at the stress levels of 115, 110, 105, 100, 85, 70, 55, and 40 percent of the material yield stress. Three stress levels higher than the material yield stress were included to detect potential fracture mechanisms due to creep deformation. The five stress levels lower than or equal to the material yield stress provided information in regard to the stress threshold level for creep initiation, as well as data required to predict long-term creep behavior.
- For the experimental tests, the temperature value of 150 °C [302 °F] was selected because, according to U.S. Department of Energy, this is the base drip shield temperature and is not expected to be exceeded during 98.5 percent of the first 10,000 years (Bechtel SAIC Company, LLC, 2004, Section 5.5). The temperature value of 250 °C [482 °F] was selected as an upper boundary for the experimental tests because the results derived by Manepally, et al. (2004) indicate that this temperature may be reached in the drip shield components if the drift collapses within several hundreds of years after the permanent closure. Moreover, creep tests were performed at room temperature—the commonly used value for this type of test—and at 100 °C [212 °F]—the temperature at which water undergoes a phase transition. Finally, a single test was conducted at 50 °C [108 °F] for 85 percent of the material yield strength for the Titanium Grade 7 as an intermediate value.

Material	Temperature °C [°F]	Tensile Strength MPa [ksi]	Yield Strength MPa [ksi]	Elongation Percent	Reduction in Area, Percent	Modulus, MPa [ksi]
HT# CN2775	25 [77]	472.9 [68.6]	361.3 [52.4]	29	52	1.06 × 10 ⁵ [1.54 × 10 ⁴]
HT# CN2775	25 [77]	475.0 [68.9]	363.4 [52.7]	29.0	47.0	1.10 × 10 ⁵ [1.60 × 10 ⁴]
HT# CN2775	50 [122]	442.6 [64.2]	337.2 [48.9]	35.5	48.0	1.10 × 10 ⁵ [1.59 × 10 ⁴]
HT# CN2775	50 [122]	437.1 [63.4]	334.4 [48.5]	41.5	49.5	1.12 × 10 ⁵ [1.63 × 10 ⁴]
HT# CN2775	100 [212]	372.3 [54.0]	281.9 [40.9]	34.5	52.5	1.16 × 10 ⁵ [1.68 × 10 ⁴]
HT# CN2775	100 [212]	366.1 [53.1]	277.2 [40.2]	37.0	54.5	1.10 × 10 ⁵ [1.60 × 10 ⁴]
HT# CN2775	150 [302]	299.2 [43.4]	226.8 [32.9]	47	61	1.01 × 10 ⁵ [1.47 × 10 ⁴]
HT# CN2775	150 [302]	288.9 [41.9]	211.7 [30.7]	35.5	58.5	1.04 × 10 ⁵ [1.51 × 10 ⁴]
HT# CN2775	250 [482]	225.5 [32.7]	166.9 [24.2]	50.0	74.5	8.89 × 10 ⁴ [1.29 × 10 ⁴]
HT# CN2775	250 [482]	233.7 [33.9]	177.9 [25.8]	55.5	68.5	8.96 × 10 ⁴ [1.30 × 10 ⁴]

Material	Temperature °C [°F]	Tensile Strength MPa [ksi]	Yield Strength MPa [ksi]	Elongation Percent	Reduction in Area Percent	Modulus, MPa [ksi]
HT# R8453	25 [77]	1108.7 [160.8]	1013.5 [147.0]	15.0	27.0	1.34 × 10 ⁵ [1.94 × 10 ⁴]
HT# R8453	25 [77]	1101.8 [159.8]	1009.4 [146.4]	13.0	27.0	1.36 × 10 ⁵ [1.97 × 10 ⁴]
HT# R8453	100 [212]	1019.7 [147.9]	892.2 [129.4]	13.0	31.0	1.30 × 10 ⁵ [1.88 × 10 ⁴]
HT# R8453	100 [212]	1021.8 [148.2]	888.0 [128.8]	14.0	37.0	1.27 × 10 ⁵ [1.84 × 10 ⁴]
HT# R8453	150 [302]	952.9 [138.2]	836.3 [121.3]	13.0	42.0	1.25 × 10 ⁵ [1.82 × 10 ⁴]
HT# R8453	150 [302]	961.8 [139.5]	835.6 [121.2]	15.0	45.5	1.28 × 10 ⁵ [1.85 × 10 ⁴]
HT# R8453	250 [482]	852.2 [123.6]	743.3 [107.8]	16.0	51.5	1.14 × 10 ⁵ [1.65 × 10 ⁴]
HT# R8453	250 [482]	845.9 [122.7]	740.5 [107.4]	13.0	56.0	1.11 × 10 ⁵ [1.62 × 10 ⁴]

- Most of the samples were subjected to short-term creep tests of 200 hours. Some of the samples with stress levels higher than 100 percent yield stress (i.e., 115, 110, and 105 percent yield stress), however, had a short creep life or broke when the load was applied.

The creep tests were performed in accordance with ASTM E-139-00 (ASTM International, 2007c).

The average yield stress of two test specimens conducted in the tensile tests was used as the 100 percent yield stress for the creep tests at a specific temperature. The creep test results at different temperatures, including stress levels, failure time, and total creep strain at the end of the tests are summarized in Table C-3 and C-4 for Titanium Grades 7 and Grade 5 alloys.

C.3 References

ASTM International. "Standard Test Methods for Tension Testing of Metallic Materials." *E-8-04: Annual Book of ASTM Standards. Vol 03.01: Metals—Mechanical Testing; Elevated and Low-Temperature Tests; Metallography.* West Conshohocken, Pennsylvania: ASTM International. 2007a.

———. "Standard Test Methods for Elevated Temperature Tension Testing of Metallic Materials." *E-21-05: Annual Book of ASTM Standards. Vol 03.01: Metals—Mechanical Testing; Elevated and Low-Temperature Tests; Metallography.* West Conshohocken, Pennsylvania: ASTM International. 2007b.

———. "Standard Test Methods for Conducting Creep, Creep-Rupture, and Stress-Rupture Tests of Metallic Materials." *E-139-06: Annual Book of ASTM Standards. Vol 03.01: Metals—Mechanical Testing; Elevated and Low-Temperature Tests; Metallography.* West Conshohocken, Pennsylvania: ASTM International. 2007c.

Bechtel SAIC Company, LLC. "Seismic Consequence Abstraction." MDL-WIS-PA-000003. Rev. 01. Las Vegas, Nevada: Bechtel SAIC Company, LLC. 2004.

Dunn, D.S., Y.-M. Pan, and K.T. Chiang. "Microstructure Analyses and Mechanical Properties of Alloy 22." CNWRA 2005-003. San Antonio, Texas: CNWRA. 2005.

Manepally, C., A. Sun, R. Fedors, and D. Farrell. "Drift-Scale Thermohydrological Process Modeling—In-Drift Heat Transfer and Drift Degradation." CNWRA 2004-05. San Antonio, Texas: CNWRA. 2004.

Table C-3. Creep Properties of Titanium Grade 7 Alloy

Material	Temperature °C [°F]	Yield Strength, MPa [ksi]	Percent of Yield Strength	Stress Level, MPa [ksi]	Time Hours	Total Creep Percent
HT#CN2775	25 [77]	362.3 [52.6]	115	417 [60.4]	8.7	28.2
HT#CN2775	25 [77]	326.3 [52.6]	110	399 [57.8]	60.0	12.9
HT#CN2775	25 [77]	362.3 [52.6]	105	380 [55.0]	200*	17.5
HT#CN2775	25 [77]	362.3 [52.6]	100	362 [52.6]	200*	5.86
HT#CN2775	25 [77]	362.3 [52.6]	85	308 [44.7]	200*	2.17
HT#CN2775	25 [77]	362.3 [52.6]	70	254 [36.8]	200*	0.43
HT#CN2775	25 [77]	362.3 [52.6]	55	199 [28.9]	200*	0.18
HT#CN2775	25 [77]	362.3 [52.6]	40	145 [21.0]	200*	0.18
HT#CN2775	50 [122]	335.8 [48.7]	85	285 [41.4]	200*	3.36
HT#CN2775	100 [212]	279.6 [40.6]	115	322 [46.6]	3.3	32.9
HT#CN2775	100 [212]	279.6 [40.6]	110	308 [44.6]	16.7	42.2
HT#CN2775	100 [212]	279.6 [40.6]	105	294 [42.6]	62.0	41.8
HT#CN2775	100 [212]	279.6 [40.6]	100	280 [40.6]	83.8	35.3
HT#CN2775	100 [212]	279.6 [40.6]	85	238 [34.5]	200*	3.02
HT#CN2775	100 [212]	279.6 [40.6]	70	196 [28.4]	200*	1.29
HT#CN2775	100 [212]	279.6 [40.6]	55	154 [22.3]	200*	0.26
HT#CN2775	100 [212]	279.6 [40.6]	40	112 [16.2]	200*	0.11
HT#CN2775	150 [302]	219.3 [31.8]	115	252 [36.6]	1.8	16.5
HT#CN2775	150 [302]	219.3 [31.8]	110	241 [35.0]	200*	1
HT#CN2775	150 [302]	219.3 [31.8]	105	230 [33.4]	10.0	14
HT#CN2775	150 [302]	219.3 [31.8]	100	219 [31.8]	200*	13.7
HT#CN2775	150 [302]	219.3 [31.8]	85	186 [27.0]	200*	2.1
HT#CN2775	150 [302]	219.3 [31.8]	70	154 [22.3]	200*	0.39
HT#CN2775	150 [302]	219.3 [31.8]	55	121 [17.5]	200*	0.17
HT#CN2775	150 [302]	219.3 [31.8]	40	88 [12.8]	200*	0.05
HT#R8453	250 [482]	172.4 [25.0]	115	198 [28.8]	200*	3.78
HT#R8453	250 [482]	172.4 [25.0]	110	190 [27.5]	200*	0.78
HT#R8453	250 [482]	172.4 [25.0]	105	181 [26.3]	0.4	0.25
HT#R8453	250 [482]	172.4 [25.0]	100	172 [25.0]	200*	4.8
HT#R8453	250 [482]	172.4 [25.0]	85	147 [21.3]	0 [†]	—
HT#R8453	250 [482]	172.4 [25.0]	70	121 [17.5]	200*	0.45
HT#R8453	250 [482]	172.4 [25.0]	55	94.8 [13.8]	200*	0.17
HT#R8453	250 [482]	172.4 [25.0]	40	68.9 [10.0]	200*	0.03

*Discontinued
[†]Machine malfunction

Table C-4. Creep Properties of Titanium Grade 5 Alloy

Material	Temperature °C [°F]	Yield Strength, MPa [ksi]	Percent of Yield Strength	Stress Level, MPa [ksi]	Time Hours	Total Creep Percent
HT#R8453	25 [77]	1011.5 [146.7]	115	1163 [168.7]	0.1*	—
HT# R8453	25 [77]	1011.5 [146.7]	110	1113 [161.4]	0.1*	—
HT# R8453	25 [77]	1011.5 [146.7]	105	1062 [154.0]	4.4	2.31
HT# R8453	25 [77]	1011.5 [146.7]	100	1012 [146.7]	200 [†]	5.36
HT# R8453	25 [77]	1011.5 [146.7]	85	860 [124.7]	200 [†]	0.04
HT# R8453	25 [77]	1011.5 [146.7]	70	708 [102.7]	200 [†]	0.03
HT# R8453	25 [77]	1011.5 [146.7]	55	556 [80.7]	200 [†]	0.05
HT# R8453	25 [77]	1011.5 [146.7]	40	405 [58.7]	200 [†]	0.23
HT# R8453	100 [212]	890.1 [129.1]	115	1024 [148.5]	0.1*	—
HT# R8453	100 [212]	890.1 [129.1]	110	979 [142.0]	0.5	1.75
HT# R8453	100 [212]	890.1 [129.1]	105	935 [135.6]	200 [†]	2.2
HT# R8453	100 [212]	890.1 [129.1]	100	890 [129.1]	200 [†]	0.55
HT# R8453	100 [212]	890.1 [129.1]	85	757 [109.7]	200 [†]	0.06
HT# R8453	100 [212]	890.1 [129.1]	70	623 [90.4]	200 [†]	0.03
HT# R8453	100 [212]	890.1 [129.1]	55	490 [71.0]	200 [†]	0.04
HT# R8453	100 [212]	890.1 [129.1]	40	356 [51.6]	200 [†]	0.02
HT# R8453	150 [302]	836.3 [121.3]	115	962 [139.5]	0.1*	—
HT# R8453	150 [302]	836.3 [121.3]	110	920 [133.4]	0.2	1.34
HT# R8453	150 [302]	836.3 [121.3]	105	878 [127.4]	0.1	—
HT# R8453	150 [302]	836.3 [121.3]	100	836 [121.3]	200 [†]	1.38
HT# R8453	150 [302]	836.3 [121.3]	85	711 [103.1]	200 [†]	0.08
HT# R8453	150 [302]	836.3 [121.3]	70	585 [84.9]	200 [†]	0.02
HT# R8453	150 [302]	836.3 [121.3]	55	460 [66.7]	200 [†]	0.04
HT# R8453	150 [302]	836.3 [121.3]	40	335 [48.5]	200 [†]	0.03
HT# R8453	250 [482]	741.9 [107.6]	115	853 [123.7]	0.1*	—
HT# R8453	250 [482]	741.9 [107.6]	110	816 [118.4]	200 [†]	0.18
HT# R8453	250 [482]	741.9 [107.6]	105	779 [113.0]	200 [†]	0.26
HT# R8453	250 [482]	741.9 [107.6]	100	742 [107.6]	200 [†]	0.14
HT# R8453	250 [482]	741.9 [107.6]	85	631 [91.5]	200 [†]	0.05
HT# R8453	250 [482]	741.9 [107.6]	70	519 [75.3]	200 [†]	0.05
HT# R8453	250 [482]	741.9 [107.6]	55	408 [59.2]	200 [†]	0.4
HT# R8453	250 [482]	741.9 [107.6]	40	297 [43.0]	200 [†]	0.26

*Sample broke when load was applied

†Discontinued